# THE ANEMOMETRIC APPLICATION OF AN ELECTRICAL GLOW DISCHARGE IN TRANSVERSE AIR STREAMS

**Thesis by**

**Ruben Fred Mettler**

**In Partial Fulfillment of the Requirements**

**For the Degree of**

**Doctor of Philosophy**

Ph D

**California Institute of Technology**

**Pasadena, California**

**1949**

ACKNOWLEDGMENT

This research was suggested by Dr. F. C. Lindvall, and was performed under the helpful supervision of Dr. Lindvall and Dr. H. W. Liepmann. The experimental work was carried out with the able assistance of Mr. A. J. A. Morgan and of several other members of Dr. Liepmann's Research Group. This supervision and assistance are gratefully acknowledged.

## Abstract

The possibility of using an electrical glow discharge for quantitative turbulence measurements is experimentally investigated. It is found that a glow discharge is stable in a transverse air stream throughout the subsonic velocity range, and at supersonic air velocities up to a Mach number of 1.5, with no indication that this Mach number represents an upper velocity limit. A calibration procedure is developed and used in measuring the decay of turbulence behind a grid at low subsonic velocities. Comparison with decay measurements made independently with a hot wire anemometer under similar flow conditions shows that the glow discharge data is as yet quite badly scattered and somewhat inconsistent.

A quantitative theory of the dark current anemometer is presented and gives results which agree in form with reported experimental results. A qualitative theory of the mechanism of the glow discharge anemometer and the first steps of the corresponding quantitative analysis are also presented.

TABLE OF CONTENTS

# I. INTRODUCTION

The study of electrical discharges in gases is still in a controversial state. Adequate physical explanations for many of the apparently significant processes occurring in both non-sustained and self-sustained discharges do not currently exist, and only a few of the processes have been explained in a universally accepted manner. Even experimental results are often not in good agreement. Consequently, it has proved very difficult to relate analytically the circuit characteristics, i.e., the current, voltage, and impedance of gas discharges to the various parameters known to affect these characteristics. Many of the features of sustained discharges in particular, have completely defied analytic description and treatment.

The situation described above is perhaps not surprising when one realizes that the circuit characteristics of a given gas discharge depend in a complicated manner upon the following variables: the atomic properties of the gas and of its impurities, the gas pressure, the gas temperature, the atomic and thermal properties of the electrode materials, the electrode configuration and shapes, the electrode spacing, the condition of the surface of the electrodes, the external circuit through which the discharge current flows, the frequency and magnitude of the driving source, and the relative velocity between the electrodes and the gas. If the effect of any one of these variables is to be studied experimentally, it is clearly necessary that all of the other variables must either be held constant or must be varied in a known and reproducible manner. In most cases, this is quite difficult. It is this

difficulty in controlling the parameters in experiments with gas discharges, that has led many able investigators to apparently conflicting experimental results. Actually, in the conflicting cases, the exact conditions were either unknown or unreported, or the experiments were not performed with sufficient care.

Even though as indicated above much fundamental research remains to be done before the physics of gas discharges is well understood, the industrial and engineering applications of gas discharge phenomena to problems such as illumination, voltage regulation, photography, air blast circuit breakers, etc. have flourished during recent years, and are widely known. The present research is aimed at furthering the development of an additional application of electrical gas discharges: namely, their use in fundamental fluid mechanics research.

An important part of the experimental research necessary to obtain an adequate working knowledge of fluid mechanics, is the development of the proper measuring instruments. This is particularly true of the study of turbulence. During the past thirty years, the development of the hot wire anemometer has steadily progressed until today it appears adequate for experimental turbulence studies at low subsonic air velocities. The chief problems associated with the hot wire anemometer are: wire strength, frequency compensation, thermal lag, and "noise-free" amplification. All of these problems become increasingly severe as the mean velocity of the air stream to be studied is increased. An instrument for measuring "turbulence" in a supersonic air stream does not currently exist. Electrical gas discharges, and in particular the glow discharge, appear to hold considerable promise for the eventual

development of an adequate instrument for measuring velocity fluctuations at supersonic speeds. Research with gas discharges tending towards the development of such an instrument will certainly also add to the knowledge and understanding of the fundamental properties and mechanisms of gas discharges in general.

The importance of the effect of the relative velocity between the electrodes and the gas of an electrical gas discharge on the circuit characteristics of the discharge, and the feasibility of using this effect to measure gas velocities, was first suggested by Lindvall in a paper published in 1934.(1) Lindvall used the voltage across a direct current glow discharge at constant current to measure mean air velocities, and showed that the voltage of such a discharge will respond to the turbulent motion in the wake of a cylinder held in a moving stream of air at atmospheric pressure. He suggested that the glow discharge anemometer might thus prove useful in the study of turbulence. No quantitative measurements of turbulence were published and no theoretical development was attempted at that time.

Late in 1941 a group of investigators in Germany became interested in Lindvall's work, and under the sponsorship of the Deutsche Versuchsanstalt Fuer Luftfahrt, began studying the use of gas discharges to measure turbulence in air. The result of their work is currently available in a series of microfilms(2) and in an NACA publication.(3) This group investigated the application of the direct current glow discharge to the measurement of turbulence in an air stream, and concluded that it is useless for such an application. Their conclusion was based upon the fact that they obtained about two (2.0) volts of noise across the

glow even at zero air velocity, and a larger noise level at higher velocities. In addition they were troubled by excessive electrode sputtering and were not able to maintain a stable glow at velocities greater than about 70 meters per second. The present author does not agree with these results, having consistently operated a direct current glow discharge with a noise level of about four thousandths (0.004) of a volt at zero air velocity, and having been able to maintain a stable discharge at a free stream air velocity of about 520 meters per second with no indication that this velocity represents an upper limit. (Since at these free stream air velocities, shock waves are formed ahead of the probe into which the electrodes are built, the velocity at the glow is less than the free stream velocity.)

Having abandoned the direct current glow discharge as a useful instrument, the attention of the German group was turned to the possibility of using a dark current discharge with a current of about a microampere or an alternating current glow discharge as an anemometer. They attempted to measure turbulence by both of these methods, using the current variations of a dark current discharge at constant voltage up to an air velocity of about 120 meters per second, and the voltage across an alternating current glow discharge at constant current up to velocities of about 50 meters per second. Their research was interrupted in 1945. No attempt was made to discuss the theory of either the direct current or the alternating current glow anemometer, and only a very sketchy and somewhat misleading theory was reported for the dark current anemometer. The evidence currently available on this dark current and alternating current glow work is not sufficient to properly

evaluate it.

There appears to be a considerable current interest at various universities in this country and in Europe, in the use of gas discharges as a means of measuring turbulence. However, at the present time (April 1949) no results have been published.

As might be expected, each of the various types of gas discharges has its own advantages and difficulties when applied as an anemometer. A discussion of those features of these discharges which significantly affect their use as anemometers is given below, based upon a survey of the references cited above, and upon experimental work presented later in this report.

The direct current glow discharge anemometer has the advantage of a convenient and easily managed current and voltage range. The current range is from two to twenty-five (2-25) milliamperes, with the voltages varying from three hundred to about seven hundred (300-700) volts, depending upon the electrode spacing, the air velocity, and the pressure. The voltage variations caused by a fluctuating air velocity are sufficient to eliminate the need for any additional amplification. In addition to simplifying the power supply problem, the low operating voltage allows the probe, into which the electrodes are built, to be made small and aerodynamically sound. A definite disadvantage of the direct current glow discharge anemometer is the electrode sputtering associated with the glow. This sputtering is not clearly understood, but qualitatively depends inversely upon the gas pressure and the electrode spacing, and directly upon the discharge current. The presence of electrode sputtering seriously complicates the calibration and operating

techniques. Another possible disadvantage of the glow discharge anemometer is the extreme difficulty in obtaining a quantitative theory to describe it.

The dark current anemometer has essentially no electrode sputtering associated with it. This is a definite advantage, and greatly simplifies the calibration and operating techniques. The theory of the dark current anemometer also appears to be simpler than that of the glow anemometer. However, the operating currents and voltages of a dark current discharge are unwieldy and difficult to manage. At voltages of from five to fifteen (5-15) kilovolts the currents vary from about one one-hundredth to about two (0.01-2.0) microamperes, depending upon the electrode spacing, the air velocity, and the pressure. These currents can be increased by a factor of three or four if the number of random electrons is increased by irradiating the electrodes with ultraviolet light or by operating the discharge in the vicinity of radioactive materials. Even so, considerable amplification is necessary, since it is the variations in this current which are of interest. These variations may be near the noise level in magnitude. The high insulation levels necessitated by the high working voltage require that the probe, into which the electrodes are built, be larger than in the case of a glow discharge. This situation is aerodynamically undesirable, particularly for high-speed work. In addition, the impedance level of the dark current discharge is so high that it is difficult to make any measurements on the circuit without materially altering the circuit characteristics.

The German group referred to above reported that the use of an

alternating current glow discharge apparently decreases the electrode sputtering, while retaining the desirable current and voltage ranges of the direct current glow discharge. However, in their work it was difficult to separate the alternating driving voltage from the components of the "turbulence voltage" in the same frequency range. The use of a driving source whose frequency is of the order of one hundred kilocycles was suggested by the German group, and represents interesting possibilities. The alternating current glow discharge was reported to be less stable in an air stream than the direct current glow.

The transitory spark discharge and the steady arc discharge appear unsuitable for anemometric purposes. A steady corona discharge might possibly be useful in this field.

The experimental work in the present research has been confined wholly to investigations with a direct current glow discharge. (Unless otherwise indicated "glow" will be taken to mean a "direct current glow" in the discussions which follow.) This type of discharge was selected because it was felt that the advantages of the easily managed current and voltage ranges, with resulting small probe size, outweighed the problems introduced by electrode sputtering, especially since possible application in the supersonic speed range was projected. The background experience gained by Lindvall in his earlier work with the glow discharge was also an important factor in the selection of this type of discharge.

## II. THEORY OF THE DARK CURRENT AND GLOW DISCHARGE ANEMOMETERS

### A. General Mechanisms

An analysis of the dark current and glow discharge anemometers will now be made to obtain theoretical equations and/or explanations which will prove useful in experimental investigations in this field. In this analysis, an attempt will be made to eliminate the non-essential features of the discharges being considered, while still retaining those processes and properties which significantly affect the characteristics of the discharge as an anemometer. The cases treated quantitatively will be considered as invariant with time, i.e., in the steady state, and will be based upon two-dimensional models. Thus the results can probably not be applied quantitatively to an actual three dimensional anemometer without some modification.

A glow discharge anemometer is operated by measuring the voltage across the discharge as the current is held constant, and as the relative velocity between the electrodes and the gas (air in this discussion) is varied. It is found (See Figure (18), for example) that in such an experiment, the voltage increases sharply with increasing air velocity. Although less convenient, a glow discharge anemometer might also be operated by holding the voltage constant and allowing the current to vary with the air velocity.

A dark current anemometer is operated by measuring the current in the electrodes of a dark current discharge operated at constant voltage as the relative velocity between the electrodes and the gas is varied. It is found that the current decreases with increasing air velocity.

The general effects of an increase in the relative velocity

between the electrodes and the gas of an electrical gas discharge will be considered, in order to determine which of these effects are predominant in causing the behavior described above. (For a general discussion of the mechanism of gas discharges in stationary gases, refer to Loeb[4], Cobine[5], or Engel and Steenbeck[6].)

As the air velocity is increased, the air pressure between the electrodes decreases slightly, the amount of pressure change depending chiefly upon the velocity increase, and upon the electrode and probe configuration. This decrease in pressure will cause the ion and electron mean free paths to increase, will change the magnitude of the ionization coefficients and will affect the diffusion and recombination processes. All of these factors have a bearing upon the voltage and current of the discharge. In the case of the glow discharge, they will cause the cathode drop region to increase in length, with an accompanying redistribution of the potential throughout the discharge.

Also, as the air velocity is increased, the heat transfer from the electrodes to the air stream is increased with a resultant cooling of the electrodes, the air stream temperature changes, and the aerodynamic forces on the electrodes and probe are altered. These effects may cause a change in electrode spacing which would be difficult to pre-calculate. The current and voltage of both the glow and dark current discharges are very sensitive to changes in electrode spacing.

The ions and electrons in a gas discharge operating in a transverse stream of air will have an average transverse component of velocity equal in direction and magnitude to the air stream velocity, unless an electric field is set up in the direction of the air flow by edge effects or by action inside the discharge. There is thus the

possibility that some of the positive ions and electrons will be blown out of the discharge, and will not reach the cathode and anode respectively. Such a loss of current carriers, or the internal action in a discharge to prevent such a loss, will affect the current and voltage of a gas discharge.

It was experimentally determined in the case of the glow discharge that the pressure changes and temperature effects associated with a change in air stream velocity do not account for the observed voltage changes. (See section (A) of part IV.) An attempt was made to design the probe used at low speeds in such a way that the aerodynamic forces caused only insignificant changes in spacing. It is the opinion of the author that the loss of positive ions is directly the cause of the current variations in the dark current anemometer, and that the observed voltage changes in the glow discharge anemometer are caused jointly by the loss of positive ions and by the internal re-distribution of the positive space charge necessary to enable the glow to sustain itself when operating in a transverse stream of air. This theory is discussed in greater detail in the two sections which follow. The loss of ions from the glow discharge was observed visually when operating the glow in a supersonic air stream.

B. Dark Current Anemometer.

In the case of the dark current anemometer, one wishes to know the current measured in the external leads attached to the anode and cathode, as a function of the transverse air velocity, when the voltage across the discharge is held constant. Only those velocities for which the accompanying pressure changes are small with respect to

the pressure at zero velocity will be considered. The changes in the anode and cathode currents with varying air velocity will be considered to be caused by the loss of those positive ions which are blown out of the discharge by the air stream. Such contributory effects as the changes in ionization coefficients caused by pressure changes, the changes in electrode spacing due to cooling of the electrodes, etc. will be neglected. An integral equation will be derived from which the distribution of electrons leaving the cathode, and hence the electron distribution throughout the discharge, can be obtained. Suitable integrations will then give us the anode and cathode currents, and the number of positive ions blown out of the discharge by the air stream.

The physical model to be used is shown in Figure (1), and represents a two-dimensional dark current discharge between two parallel

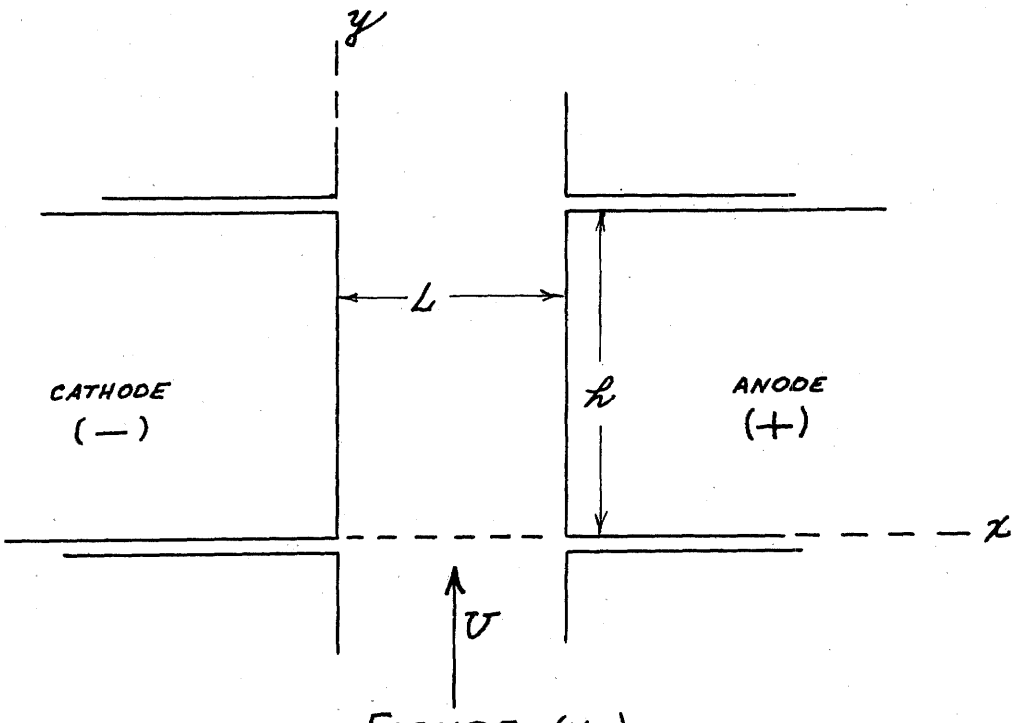


FIGURE (1)

closely spaced electrodes of width h and separation L. For convenience, a thickness of one centimeter will be assumed. A uniform transverse air velocity U is taken as acting in the direction of the positive y-axis. All viscous effects will be neglected. The field between the electrodes will be considered as being uniform. The edge effects are thus neglected and it is implied that the space charge is small enough to cause only negligible field distortion.

A dark current discharge is not self-sustained, and requires a continuous source of excitation from outside the discharge itself if the current is to be continuous. This external excitation will be considered to be such that it causes a constant number, $n_o$, of electrons to leave each square centimeter of the cathode each second. These electrons will travel towards the anode with a drift velocity $\mu_e E$, where $\mu_e$ is the electron mobility and $E$ is the field strength, and will gain enough energy from the field to ionize gas molecules by "collision". The positive ions so formed will then travel towards the cathode with a drift velocity $\mu_p E$ where $\mu_p$ is the mobility of the positive ions and $E$ is again the field strength. Upon striking the cathode the positive ions will, on the average, cause $\gamma n_p$ electrons to be emitted per square centimeter per second, where $n_p$ is the number of positive ions striking each square centimeter of the cathode per second, and $\gamma$ is a proportionality constant which depends upon the energy of the positive ions, the field strength at the cathode, the cathode material, and the conditions of the cathode surface. These electrons are in addition to those leaving the cathode due to the external excitation, so that the total number of electrons leaving each square

centimeter of the cathode per second is given by,

$$n_c = n_o + \gamma n_p \qquad (1)$$

The improbable process of ionization by positive ions by "collision" will not be considered.

The case in which the transverse air velocity is zero will be considered first. In the steady state, neglecting recombination and diffusion, the number of positive ions striking each square centimeter of the cathode per second at zero air velocity must be equal to the total number of new ions being produced per second in a volume perpendicular to the electrode surfaces, with a one square centimeter cross-sectional area and a length of $L$ units in the $x$ direction. Conditions at the cathode at zero velocity are independent of $y$. The number of new ions (and electrons) produced per second in any length $dx$ of this volume is given by

$$dn_p = \alpha n_e(x)\, dx \,, \qquad (2)$$

where $n_e(x)$ is the number of electrons per second which cross one square centimeter in a plane at a distance $x$ from the cathode, and the proportionality constant $\alpha$ is the familiar first Townsend coefficient which depends primarily upon the field strength, the pressure, and the type of gas involved. This expression neglects recombination, diffusion, and the improbable process of ionization by positive ions. The total number of positive ions per square centimeter per second striking the cathode is therefore given by

$$n_p = \int_0^L \alpha n_e(x)\, dx \,. \qquad (3)$$

Upon integrating equation (2) one obtains,

$$n_e(x) = n_c\, e^{\int_0^x \alpha\, dx} \tag{4}$$

which, upon substituting into equation (1), yields,

$$n_c = n_o + \gamma \int_0^L \alpha\, n_c\, e^{\int_0^x \alpha\, dx}\, dx \tag{5}$$

Under the assumption that the field strength $E$ is a constant, the coefficient $\alpha$ may be treated as a constant for the small pressure changes considered here, and the integration indicated in equation (5) is easily performed. Solving the integrated expression for $n_c$, one obtains,

$$n_c = \frac{n_o}{1 - \gamma\,(e^{\alpha L} - 1)} \quad . \tag{6}$$

Applying equation (4), one thus has the number of electrons per square centimeter per second crossing a plane a distance x from the cathode,

$$n_e(x) = \frac{n_o\, e^{\alpha x}}{1 - \gamma\,(e^{\alpha L} - 1)} \tag{7}$$

The electron distribution throughout the discharge in this case increases with x and is independent of y. As expected there is a direct dependence upon $n_o$ , the number of electrons produced by the external excitation, without which the entire discharge current would vanish.

When the anemometer is in operation, with a transverse air velocity of magnitude U, the drift paths of the ions and electrons are different from those in the above case, and hence equations (7) no longer applies. The electrons will be assumed to travel along paths perpendicular to the electrode surfaces, while the positive ions travel

along paths inclined to the electrode surfaces by an angle $\phi$ which is given by

$$\phi = \tan^{-1}\left(\frac{v}{\mu_p E}\right). \tag{8}$$

This is illustrated in Figure (2).

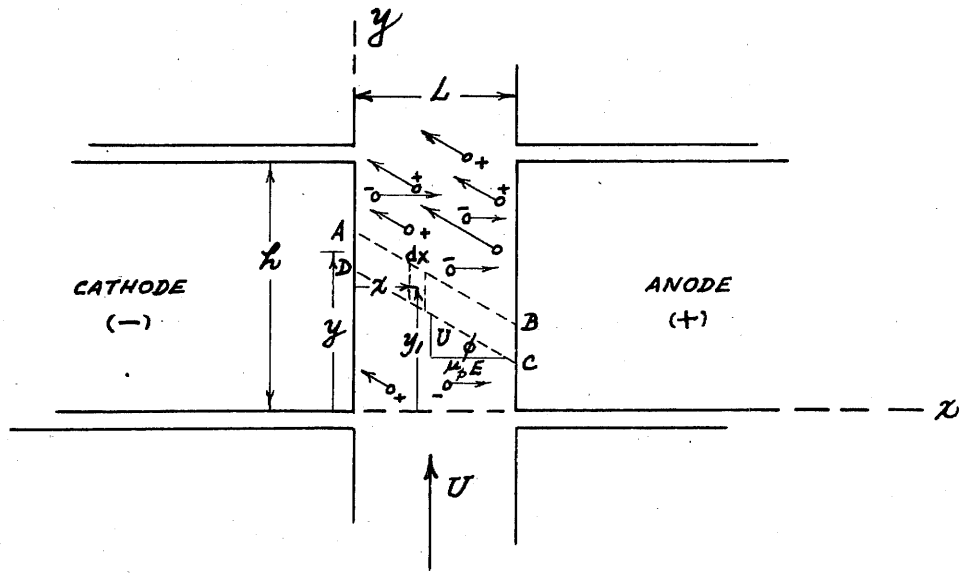


FIGURE (2)

If the drift velocities of the positive ions and of the electrons for a typical electrode spacing and a typical operating voltage are compared, it will be seen that such an assumption is reasonable. (Using the mobility data given by Loeb[7], and taking as an example, a spacing of 4 millimeters, and a voltage of 6000 volts, one obtains about 240 meters per second as the drift velocity for the positive ions, and about 83,000 meters per second as the drift velocity of the electrons, under the previous assumption of uniform field strength. Thus the drift velocity of the electrons is about 350 times as great as that of the positive ions, and at the air stream velocities under consideration here, the electrons

arrive at the anode without having been appreciably deflected. The amount of electron diffusion in the y-direction during the very short electron transit time is also negligible.)

With the transverse velocity $v$ acting upon the discharge, equation (1) is replaced by,

$$n_c(y) = n_o + \gamma n_p(y) \tag{9}$$

where $n_c$ and $n_p$ are functions of y. In the steady state, again neglecting recombination and diffusion, $n_p$ at any value of y is just the number of new ions produced per second by electron "collisions" in a volume such as ABCD of Figure (2).

The number of new ions produced per second in any length $dx$ of this volume, is $\alpha n_e(x, y_1)$ where $n_e(x, y_1)$ is the number of electrons per second which cross one square centimeter at $(x, y_1)$. Since the electrons are assumed to drift in the x- direction, equation (4) is still applicable and under the assumption of uniform field one obtains,

$$n_e(x, y_1) = n_c(y_1)\, e^{\alpha x} . \tag{10}$$

The total number of new ions produced per second in the volume ABCD of Figure (2) is thus,

$$n_p(y) = \int_0^L \alpha\, n_c(y_1)\, e^{\alpha x}\, dx , \tag{11}$$

which gives for equation (9),

$$n_c(y) = n_o + \gamma \int_0^L \alpha\, n_c(y_1)\, e^{\alpha x}\, dx . \tag{12}$$

This integral equation can be put in a more convenient form by retaining

only the variables $y$ and $y_1$. Using the expressions

$$x = \frac{\mu_p E}{U}(y - y_1)$$
$$dx = -\frac{\mu_p E}{U} dy_1 \tag{13}$$

and appropriately changing the limits,

$$n_c(y) = n_o + \gamma \int_{y - \frac{Ul}{\mu_p E}}^{y} \frac{\alpha \mu_p E}{U} n_c(y_1) e^{\frac{\alpha \mu_p E}{U}(y - y_1)} dy_1 , \tag{14}$$

where, under the above assumptions, $\alpha$, $\mu_p$, $E$ and $\gamma$ are constants. (The theory proposed by W. Fucks[8] neglected the secondary electrons produced by ions striking the cathode. It appears that such an assumption is not warranted. It is clear that in equation (14) such an assumption is equivalent to setting $\gamma$ equal to zero, and hence reduces $n_c(y)$ to the constant $n_o$.) From equation (14), one can find $n_c(y)$, which must clearly be finite and continuous in the range $o < y < h$, must reduce to $n_o$ when $y$ is zero, and must be zero for negative values of $y$. The solution of this integral equation is quite interesting and is included as Appendix A.*

For values of $y$ in the range $o < y < \frac{Ul}{\mu_p E}$, the solution is,

$$n_c(y) = \frac{n_o}{1+\gamma}\left\{1 + \gamma e^{\frac{\alpha \mu_p E}{U}(1+\gamma)y}\right\} \tag{15}$$

---

*The author is indebted to Dr. C. R. DePrima for suggestions on the solution of this equation.

and for $\frac{Vl}{\mu_p E} < y < \frac{2Vl}{\mu_p E}$ the solution is,

$$n_c(y) = \frac{n_o}{1+\gamma} + \frac{n_o \gamma e^{\alpha l}}{(1+\gamma)^2} + \left\{ \frac{n_o \gamma}{1+\gamma} - \frac{n_o \gamma e^{-\gamma\alpha l}}{(1+\gamma)^2} + \frac{n_o \gamma^2 \alpha l e^{-\gamma\alpha l}}{1+\gamma} \right\} e^{\frac{\alpha \mu_p E}{V}(1+\gamma)y}$$

$$- \frac{n_o \gamma^2 \alpha \mu_p E\, e^{-\gamma\alpha l}}{V(1+\gamma)}\, y\, e^{\frac{\alpha \mu_p E}{V}(1+\gamma)y} \qquad (16)$$

These expressions can be checked by direct substitution into the original integral equation. Solutions for $y > \frac{2Vl}{\mu_p E}$ can also be obtained by applying the method developed in Appendix A.

One can now obtain an expression for the currents measured in the anode and cathode leads as illustrated by Figure (3).

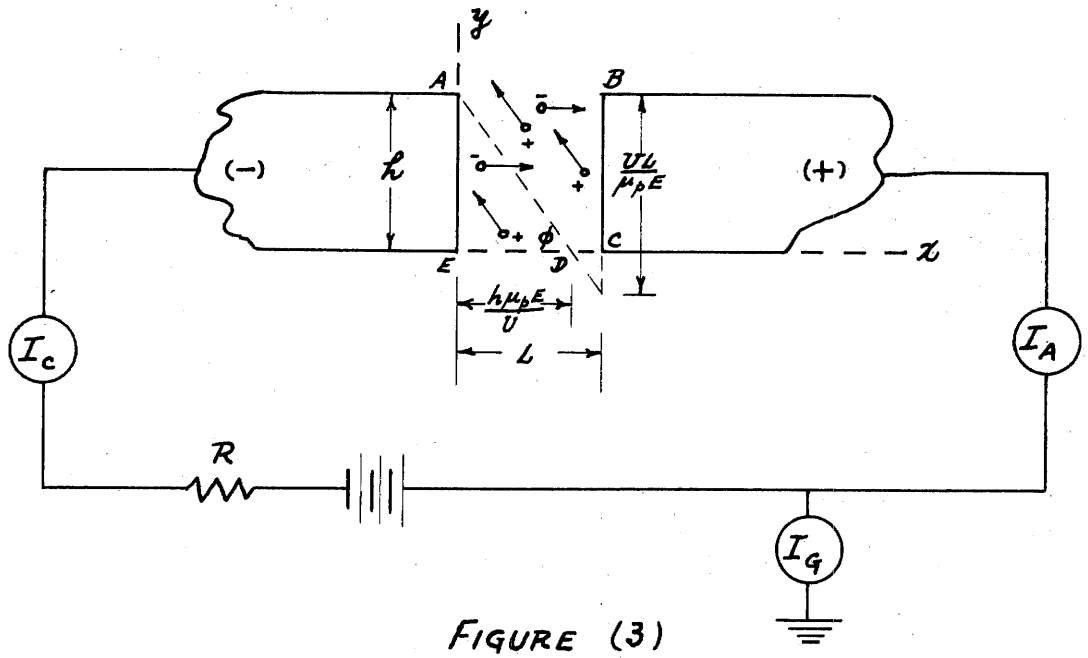


FIGURE (3)

The current in the anode lead is given by the number of electrons which arrive at the anode per second multiplied by the charge per electron. From equation (10), the number of electrons per square centimeter arriving at any point on the anode per second is given by

$n_c(y)\, e^{\alpha L}$, and hence,

$$I_A = g e^{\alpha L} \int_0^h n_c(y)\, dy \quad , \tag{17}$$

where the integration is performed in steps of $\frac{VL}{\mu_p E}$ (See Appendix A) if necessary in order to cover the range from zero to h. The current in the cathode lead is given by the number of electrons leaving the cathode per second multiplied by the charge per electron plus the number of positive ions striking the cathode per second multiplied by the charge per ion. The cathode current is thus,

$$I_c = (I_c)_e + (I_c)_p \tag{18}$$

$$I_c = g \int_0^h n_c(y)\, dy + g \int_0^h n_p(y)\, dy \,. \tag{19}$$

Substituting from equation (9) for $n_p(y)$,

$$I_c = g \frac{\gamma+1}{\gamma} \int_0^h n_c(y)\, dy - \frac{n_o h g}{\gamma} \tag{20}$$

where the integration is again broken up into steps of $\frac{VL}{\mu_p E}$ if necessary in order to cover the range from zero to h. The integration indicated by equations (17) and (20) is performed for a given case in Appendix B; a discussion of the current $I_G$ which flows in the ground wire is also given there. An interesting check of this method of obtaining the anode and cathode currents can be made by applying equations (17) and (20) to the case where the air velocity is zero. The result is

$$I_A = I_c = \frac{n_o h g e^{\alpha L}}{1 - \gamma(e^{\alpha L} - 1)} \equiv I_o \tag{21}$$

which shows the two currents equal as they are known to be in the zero velocity case.

By comparing equation (19) and (20) one can write,

$$I_c = \frac{\gamma+1}{\gamma e^{\alpha L}} I_A - \frac{n_0 h g}{\gamma} \qquad (22)$$

This equation can be put in a useful dimensionless form by dividing by the current for zero velocity as given by equation (21), giving

$$\frac{I_c}{I_o} = 1 - \frac{\gamma+1}{\gamma e^{\alpha L}} \left(1 - \frac{I_A}{I_o}\right) \qquad (23)$$

where the ratios $\frac{I_c}{I_o}$ and $\frac{I_A}{I_o}$ are known as a function of velocity from equations (17), (20) and (21), and are evaluated for a given case in Appendix B. This result can be interpreted more readily if equation (23) is put in the following form:

$$\left(1 - \frac{I_c}{I_o}\right) = \frac{\gamma+1}{\gamma e^{\alpha L}} \left(1 - \frac{I_A}{I_o}\right) \qquad (24)$$

The quantity $\frac{\gamma+1}{\gamma e^{\alpha L}}$ on the right side of this expression has a magnitude

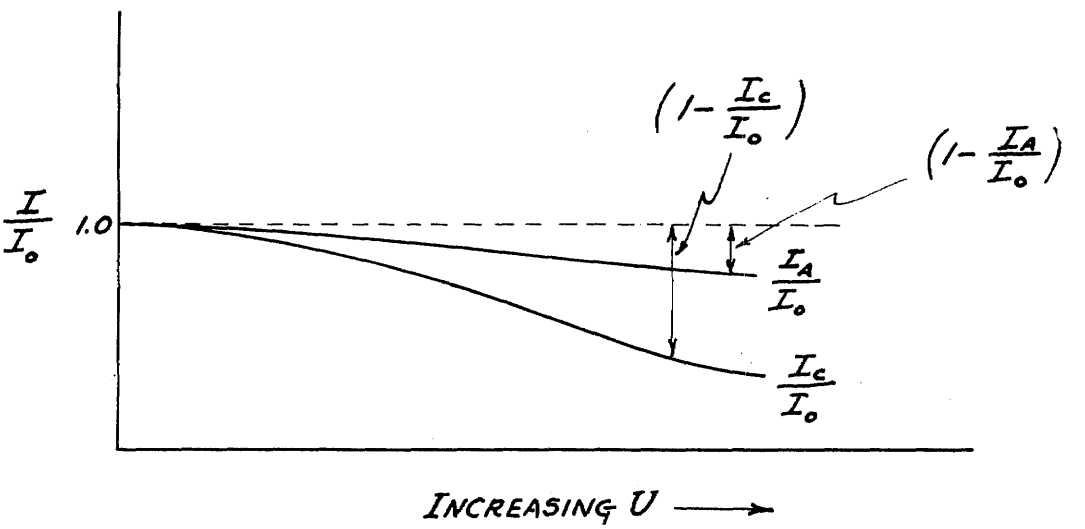


FIGURE (4)

greater than one for the values of spacing, field strength, air pressure, and for the electrode materials used in dark current anemometer measurements. The ratio $\frac{I_A}{I_o}$ decreases with increasing air velocity. Hence, using equation (24), the relative variation of $I_A$ and $I_c$ can be sketched as a function of air velocity. (Figure (4).)

The dependence of $I_A$ and $I_c$ upon velocity as derived theoretically in the above work and as sketched in Figure (4), is of the same form as the experimental dependence of $I_A$ and $I_c$ upon velocity obtained and reported by Kettel[9]. A direct numerical comparison with experiment can not be made at this time because the exact constants and dimensions which apply to Kettel's experiments are not available. However, since the theoretical results agree in form with experiment, it is believed that the theory presented is essentially correct, and that the effects which were neglected are of second order importance.

The difference between $I_A$ and $I_c$ illustrated in Figure (4) depends directly upon the number of ions blown out of the discharge. (See Appendix B.) This loss of ions also determines the decrease in $I_A$, since it results in a smaller number of impacting ions at the cathode, and hence in a smaller number of secondary electrons being ejected at the cathode. Thus, even though the assumption that the electrons are not deflected by the air stream was made, the number of electrons arriving at the anode decreases with increasing velocity.

The above analysis was based upon steady state conditions. In turbulence research, one is generally most interested in the fluctuating components of velocity, and hence in the dynamic response of the discharge. The transit time of the electrons is of the order of a

twentieth of a micro-second and the transit time of the ions is of the order of ten to thirty microseconds, both depending upon the applied voltage and the electrode spacing. For measuring turbulence velocities, whose principal frequency components lie below ten thousand cycles per second, the spacing and voltage could be adjusted to make the ion transit times about one-tenth as great as the shortest period of air velocity fluctuations. It therefore appears valid to assume that the derived or experimentally obtained steady state characteristics may be applied in the calibration for dynamic measurements.

C. Glow Discharge Anemometer

As a part of this study, an attempt was made to obtain a theoretical expression for the voltage-velocity characteristic of the glow discharge anemometer similar to that developed for the current-velocity characteristic of the dark current anemometer. This effort has thus far been successful only in that a few general quantitative relations and a qualitative theory of the mechanism of the glow discharge anemometer have been developed. This treatment of the glow discharge is admittedly approximate and the effects of some of its features, such as the anode spot and anode drop are simply omitted as being less important than the features considered. All effects of viscosity are neglected. The same notation and coordinates used in discussing the dark current discharge will be used here.

The mechanism of a glow discharge is much more complex than that of a dark current discharge. A glow discharge sustains itself without any random external excitation such as was assumed to be acting upon the cathode in the dark current discharge. Any analysis of the

glow must be consistent with this self-sustaining property. The basic simplifying assumption which was made in treating the dark current discharge, and which made that case soluble, was the assumption that the electric field was uniform. This implied that the currents were so small that the space charge distortion of the field was negligible. In the glow discharge, the field distortion caused by the space charge is an inherent part of the sustained operation of the glow, and the assumption of uniform field is clearly not valid.

In order for a glow discharge to be established, conditions must be such that any random electrons and/or ions which enter the space between the electrodes will initiate regenerative secondary processes which result in the current increasing from zero to the sustained value necessary for a stable glow discharge. The most important secondary processes, and the only ones which we will consider in this discussion, are ionization by electrons by "collision", and the release of electrons at the cathode by positive ion bombardment. Once the glow discharge is established, the number of electrons leaving the cathode as a result of random external excitation is entirely negligible compared with the number released by positive ion bombardment, and the random excitation is no longer significant. It is clear that if the magnitude of the glow discharge current is to remain constant, any given number of electrons leaving the cathode must cause a chain of events which, on the average, will just replace that number of electrons at the cathode. We can, therefore, write the "continuity" relation,

$$\int_0^h n_c(y)\,dy = \int_0^h \gamma(y)\, n_p(y)\,dy \qquad (25)$$

where $n_c(y)$ is the number of electrons leaving the cathode at y per square centimeter per second, $n_p(y)$ is the number of positive ions striking the cathode at y, per square centimeter per second, and $\gamma$ now also depends upon y. Equation (25) can be re-written,

$$\int_0^h n_c(y)\,dy = \gamma_{EFF.}\left\{\int_0^h n_A(y)\,dy - \int_0^h n_c(y)\,dy - N_L\right\} \qquad (26)$$

where the entire bracket on the right side represents the number of positive ions striking the cathode and $\gamma_{effective}$ is a constant relating the number of electrons released from the cathode to the number of ions striking it. The terms inside the bracket are interpreted as follows: the term $\int_0^h n_A(y)\,dy$ represents the number of electrons reaching the anode per second, the term $\int_0^h n_c(y)\,dy$ represents the number of electrons leaving the cathode per second, and $N_L$ is the number of positive ions blown out of the discharge per second by the transverse air stream. The difference of the first two terms in the bracket is, clearly, the total number of positive ions produced per second, minus the number "lost" by recombination and diffusion per second. It will be observed that this implies that all of the free electrons reach the anode, even though some positive ions do not reach the cathode.

The number of ions (and electrons) "lost" by recombination is very difficult to evaluate. In the case of the dark current discharge, it appeared valid to neglect recombination. In the glow discharge case, recombination appears to be more important; however, one would probably neglect it as a first approximation. The further evaluation of the terms in equation (26) depends upon a knowledge of the field strength and of the paths of the electrons and positive ions

inside the discharge.

It can easily be shown that the paths of the ions and electrons in the glow discharge anemometer cannot be the simple straight lines used in the dark current analysis. Consider Figure (5), where the discharge is two dimensional, and imagine for the moment that the electrons drift only in the $x$-direction and that the ions follow paths inclined to the x-axis by the angle $\phi$ previously defined by equation (8). Then a group of electrons leaving a typical point such as A will produce ions by "collision" along the line AB. These ions will drift along the inclined paths and will strike the cathode at points such as C, where more electrons are released. These electrons drift along lines such as CD, etc. etc. It is clear that with such ion and electron paths, the electrons which left point A would not be replaced, and the discharge could not sustain itself. Therefore, the assumption of straight line paths is not applicable to the glow discharge anemometer. In fact, it is clear that the ions produced by the electrons leaving point A, for example, must have forces acting upon them in the upstream direction during part of their path, in order that at least some of them can travel upstream against the velocity U and arrive at point A, where they produce the requisite number of electrons to sustain the discharge.

The positive space charge in the cathode drop region provides a means by which the ions can be turned upstream. Consider Figure (6), where the edge effects have not been ruled out, and imagine that to begin with, a stable glow discharge is operating at zero velocity. The ion and electron drift paths are then essentially along the $x$ axis,

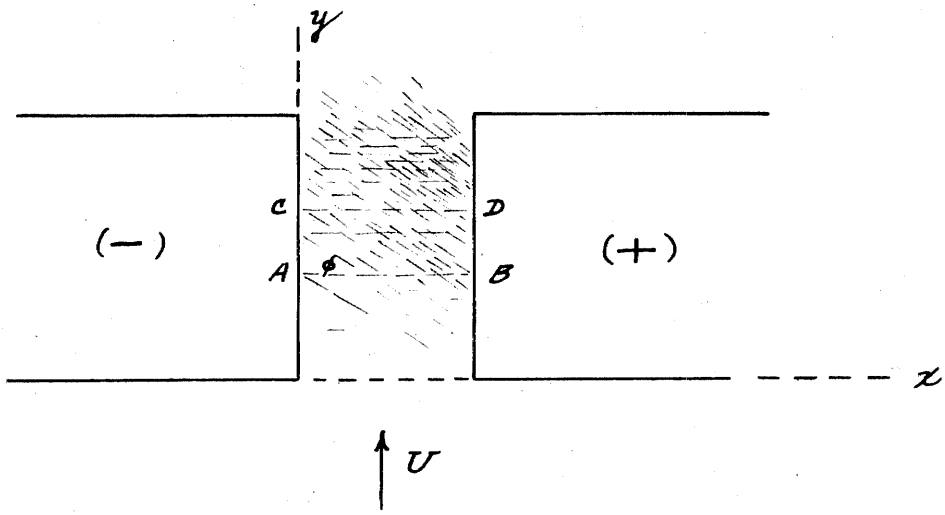


FIGURE (5)

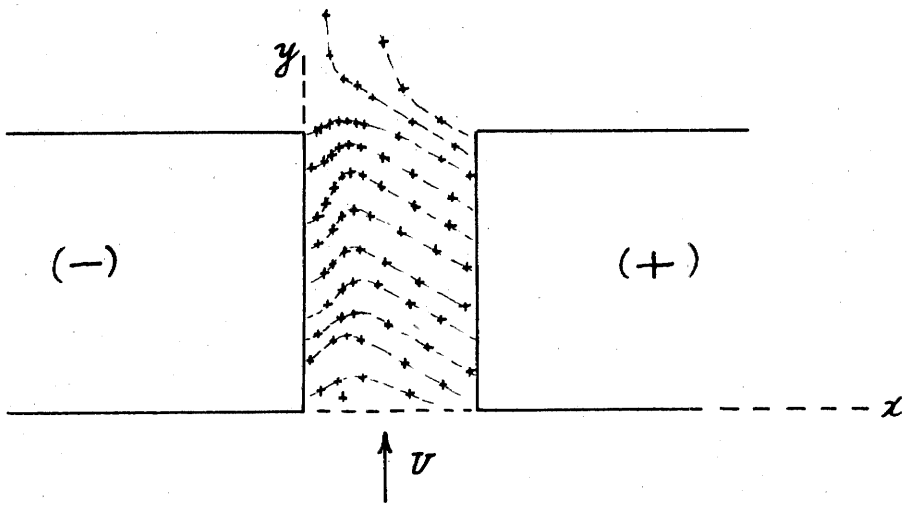


FIGURE (6)

and the positive ion space charge in the cathode drop region will be uniformly distributed in the y direction. This space charge results of course from the lower ion velocities in that particular region. Now if a transverse air velocity U is suddenly established, the ions will strike the cathode at points further in the positive y direction than they would have if the velocity U were not present. The current density and hence the concentration of the space charge will, therefore, increase at the larger values of y. However, as a gradient is set up in the space charge concentration, an electric field is established in the negative y direction. This field acting upon the positive ions, plus diffusion of positive ions in the space charge in the negative y direction made possible by the concentration gradient, cause the ions to move upstream in the vicinity of the space charge. The edge effects near the downstream edge of the electrodes also provide a local upstream field component. When the steady state is reached, the concentration gradient in the space charge is just sufficient to force the necessary number of positive ions upstream to points on the cathode where they will produce the electrons necessary to sustain the discharge. Some positive ions are blown out of the discharge. Figure (6) indicates what the average paths of the positive ions might look like. Of course, in an actual discharge, this picture is complicated by the fact that there may be a small negative space charge on both sides of the positive space charge which will tend to reduce the effects of the positive space charge; the fields set up by these space charges will act upon the electrons as well as upon the ions and will provide the electrons with a downstream component of motion.

Intuition suggests that the internal redistribution of the space charge can never completely compensate for the effects of the air stream which caused the redistribution. By examining the discharge through a microscope as the velocity is increased, one observes that this is actually the case, and that the discharge moves slightly downstream with each velocity increase, covering increasingly less of the cathode area. Therefore, if the current is kept constant, the current density of the discharge must increase. The voltage must then go up, in order to replace the ions lost, and in order to allow the discharge to operate in its "abnormal" state at the increased current density.

Returning now to equation (25), we see that, on the average in the steady state, the "continuity" relation for a sustained discharge must hold at all points along the cathode, so that we can write,

$$n_c(y) = \gamma(y)\, n_p(y) \qquad (27)$$

This equation is analogous to equation (9) in the dark current analysis. Let us consider Figure (7), where typical ion and electron drift paths are sketched. Since the mean free paths of the ions are very small compared to the electrode dimensions, one can consider that on the average in the steady state, all of the ions produced along a path such as AB will drift along AB and strike the point A. At a typical point A, the number $n_p(y)$ of positive ions striking the cathode per square centimeter per second is approximately equal to the number of ions produced per second along the path AB by electron collisions. The number of positive ions produced per unit volume per second at any point such as $P$ along the path AB by electron "collisions" is, neglecting

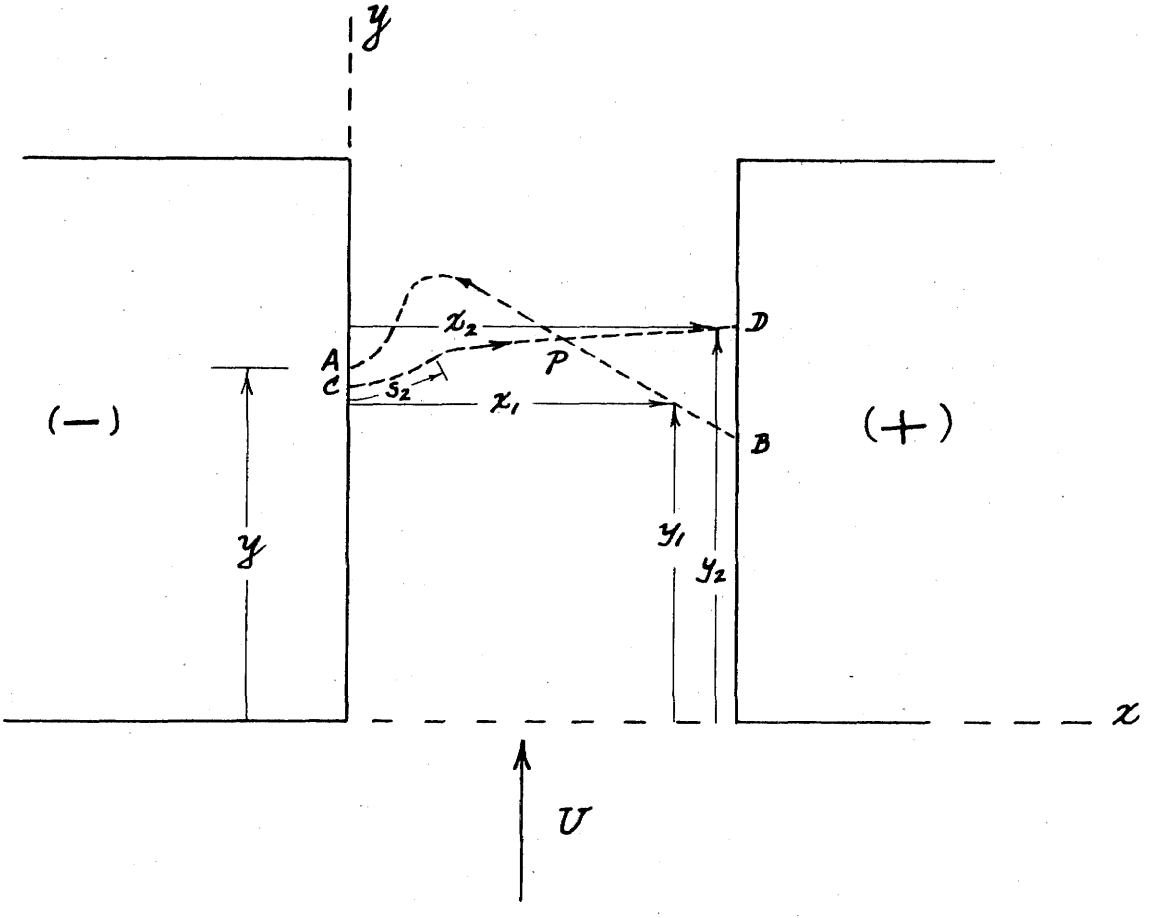


FIGURE (7)

recombination and diffusion,

$$dn_p = \alpha(x_1, y_1)\, n_e(x_1, y_1)\, ds_2 \tag{28}$$

where $\alpha(x_1, y_1)$ is the ionization coefficient at a point such as $\mathcal{P}$, $ds_2$ is an element of length along an electron path such as CD which intersects the path AB at $\mathcal{P}$, and $n_e(x_1, y_1)$ is the number of electrons which pass a unit area perpendicular to the electron path per second at a point such as $\mathcal{P}$. The quantity $n_e(x_1, y_1)$ depends upon the number of electrons leaving point C and upon the integrated effect of $\alpha(x_2, y_2)$ from C to $\mathcal{P}$. In any length $ds_2$ along the electron path CD, we can write for the number of new electrons produced,

$$dn_e = \alpha(x_2, y_2)\, n_e(x_2, y_2)\, ds_2 \tag{29}$$

which can be integrated to,

$$n_e(x_1, y_1) = n_c(y_2)\, e^{\int_C^{\mathcal{P}} \alpha(x_2, y_2)\, ds_2} \tag{30}$$

Equation (27) can now be given as, using equation (28),

$$n_c(y) = \gamma(y) \int_A^B dn_p = \gamma(y) \int_A^B \alpha(x_1, y_1)\, n_e(x_1, y_1)\, ds_2 \tag{31}$$

which by substituting equation (30) becomes

$$n_c(y) = \gamma(y) \int_A^B \alpha(x_1, y_1)\, n_c(y_2)\, e^{\int_C^{\mathcal{P}} \alpha(x_2, y_2)\, ds_2}\, ds_2 \tag{32}$$

which is an integral equation for $n_c(y)$ analogous to the integral equation for $n_c(y)$ (equation (12)) which was solved in the dark current

case. The difficulty in proceeding with the solution of equation (32) is now apparent. It would be necessary to put equation (32) in a form analogous to equation (14); that is, eliminate the variables $x_1$, $x_2$ and $S_2$ and retain only $y$, $y_1$, and $y_2$. This would require a knowledge of the paths AB and CD, which clearly depend in turn in a very complex way upon the distribution of space charge and hence upon $n_c(y)$, which is our unknown. In addition, since $\alpha$ is a function of the electric field strength and the air pressure, the field strength must be determined in terms of $n_c(y)$.

A reasonable first simplification might be to assume that the electrons drift only in the x-direction. Under such an assumption, there is then no need to consider the running variables $x_2$ and $y_2$, and one obtains for equation (32) the simplified form,

$$n_c(y) = \gamma(y) \int_0^L \alpha(x, y_1)\, n_c(y_1)\, e^{\int_0^x \alpha(x, y_1)\, dx}\, dx \qquad (33)$$

In order to put this equation in a form similar to equation (14), a knowledge of the path AB and a relation between $\alpha(x, y_1)$ and $n_c(y)$ are still required. The solution of even the simplified form given by equation (33) is therefore still very difficult.

Equation (32) expresses the self-sustained nature of the glow discharge. In addition we know that: the potential distribution in the discharge must satisfy Poisson's equation; the field strength integrated along any path from cathode to anode must yield the same value for the potential difference across the discharge; the positive ion velocities in the x- and y-directions are $\mu_p E_x$ and $\mu_p E_y$, where $\mu_p$

depends in an experimentally known way upon the ratio of field strength to gas pressure; the electron velocities in the x- and y-directions are $\mu_e E_x$ and $\mu_e E_y$, where $\mu_e$ also depends upon field strength and gas pressure; the quantity $\gamma(y)$ depends upon the energy of the positive ions, the field strength at the cathode, the gas and the cathode material, and the condition of the cathode surface, and could probably be determined by experiment. In principle, this information should allow one to determine the ion and electron paths and $\alpha(x, y)$, and thus put equation (32) in a form where it could be solved for $n_c(y)$. A knowledge of $n_c(y)$ would allow one to calculate expressions for the currents in the anode and cathode leads as functions of the air velocity at constant voltage. Such expressions could then be solved to give the voltage as a function of velocity at constant current.

An analysis such as is indicated above, if it could be completed, would probably not check an actual glow discharge anemometer experiment very well. This would be expected, since we have omitted all three-dimensional effects, all viscosity effects, all effects of sputtering, all recombination and several features of the glow such as the anode spot and anode drop phenomena. The operating characteristics of a particular glow discharge anemometer must clearly be determined experimentally.

None of the above steady state discussion throws any light upon the dynamic response of the glow discharge to a fluctuating air velocity. From a consideration of the transit times in the dark current case, we could estimate the velocity fluctuation frequency below which the current faithfully follows the velocity variations. In the

glow discharge case, the dynamic behavior involves changes in space charge density and the shifting of the space charge in a complicated way. This makes even an estimate of frequency response quite difficult. However, an experimental indication of the frequency response was given by Phillips(10). He built a glow discharge microphone which was used in actual commercial broadcasting for a short time. He reported that the frequency response could be improved by decreasing the length of the positive column; the positive column decreases as the spacing is decreased. For a spacing greater than the spacings used in the glow discharge anemometer, he estimated the frequency response to be flat to better than four thousand cycles per second. Unfortunately, he did not give any curves or other quantitative data on the operation of his glow discharge microphone. Since the spacings used in the glow discharge anemometer can be made short enough to eliminate the positive column entirely, one would expect the frequency response to be flat to considerably better than four thousand cycles per second.

## III. DESCRIPTION OF EXPERIMENTAL APPARATUS

A general picture of the experimental apparatus used will first be presented, followed by a detailed description of the more important features of the apparatus. The data obtained with each of these experimental setups are presented in the next section of this thesis.

The experimental work associated with this research was concerned only with the direct current glow discharge anemometer, operated with the anode current held constant. The electrical circuit used is given in Figure (8). It will be observed that this circuit is very simple, consisting only of a power supply, current regulator, and the measuring circuits, in addition to the glow discharge itself. Care was taken to provide adequate insulation and protection in the high voltage portion of the circuit.

The actual physical arrangement of this circuit with the side panels removed is shown in Figure (9). The bottom compartment of the cart contains the power supply, the second compartment contains the current regulator, and the measuring instruments are on the top.

The moving air stream was obtained in several different ways as the experiments progressed. The initial setup was designed to determine in a quick and only approximate manner the air velocity range and the current range through which one could maintain a stable glow discharge at near atmospheric pressure. For this purpose the electrodes were simply insulated and inserted into the throat of a converging nozzle, whose throat diameter was 3/16 of an inch and which discharged to the atmosphere. The nozzle was supplied through a stagnation chamber and a large storage tank from a compressor of suitable capacity. Throttling and

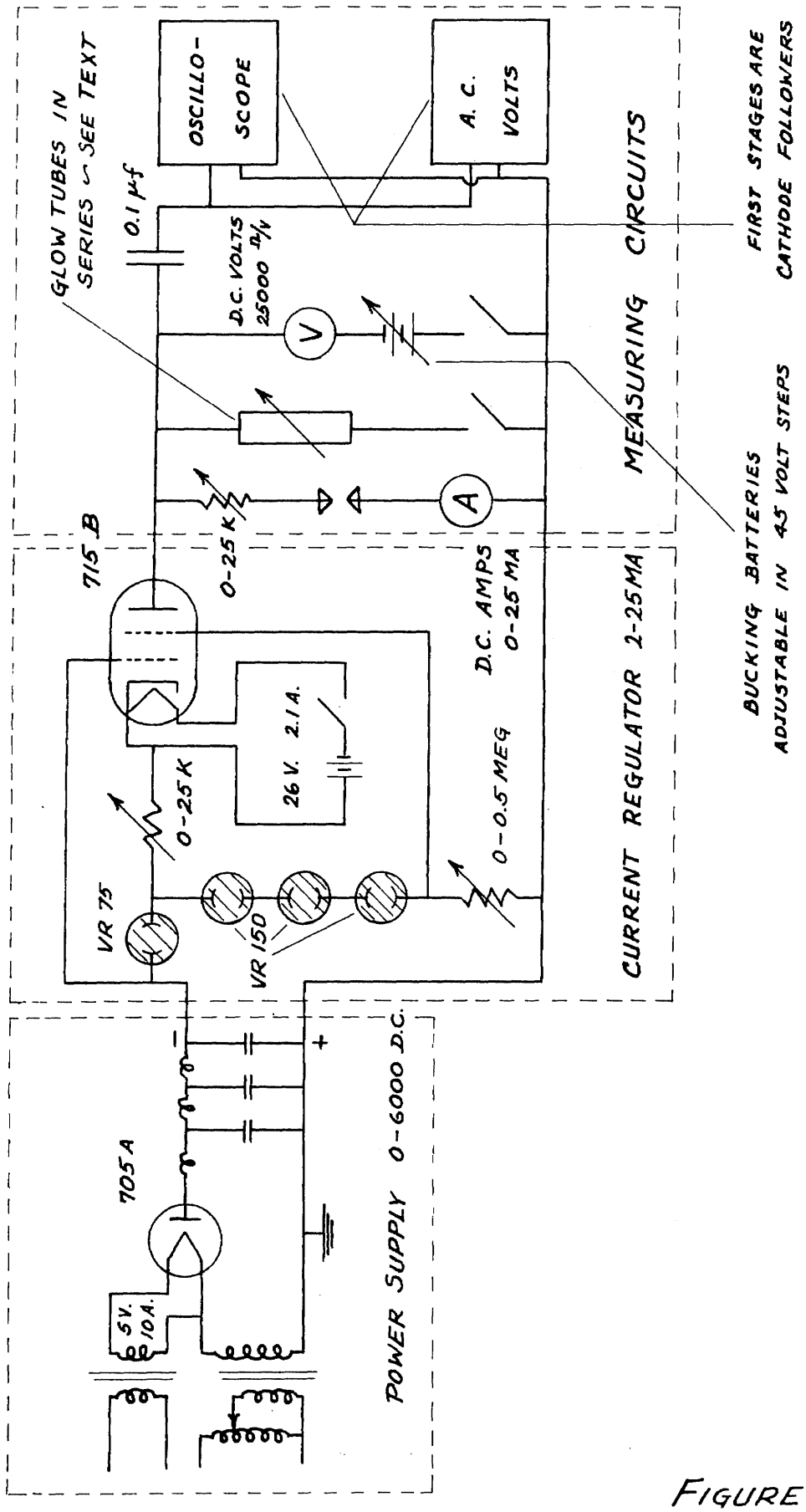


FIGURE (8)

GLOW DISCHARGE ANEMOMETER CIRCUIT

FIGURE (8)

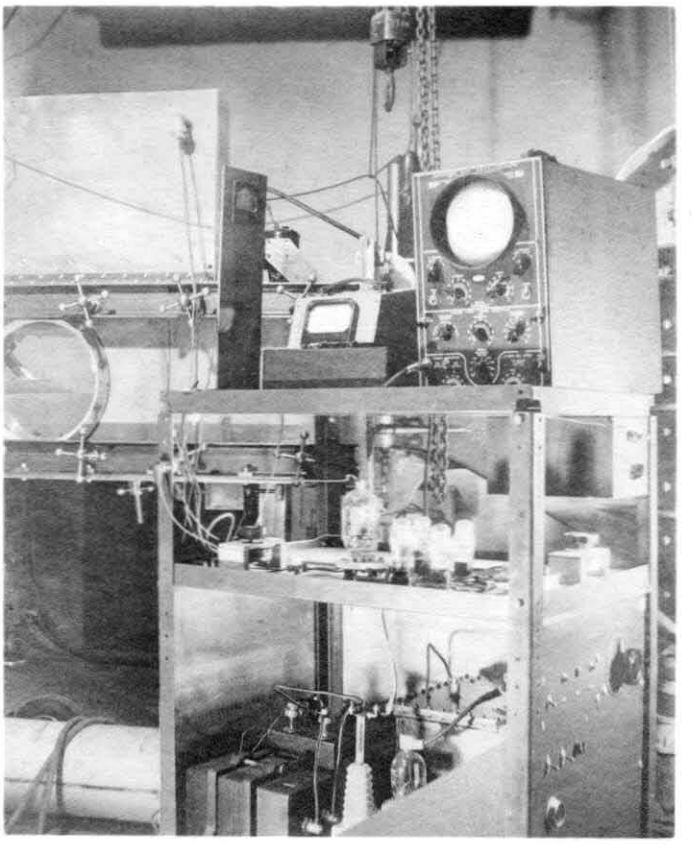

POWER SUPPLY

Figure (9)

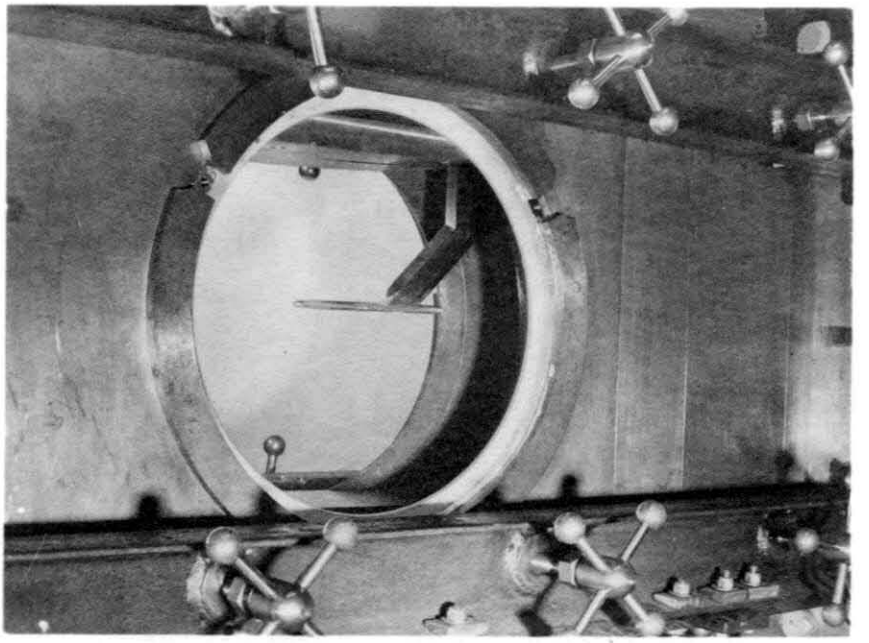

PROBE MOUNTED IN TEST SECTION

Figure (10)

bleeding valves were provided so that the pressure just ahead of the nozzle could be set at a constant value. Provision was made for observing the glow through a microscope while it was in the air stream.

After the preliminary survey data were taken, the glow discharge anemometer was operated at low subsonic velocities in the GALCIT 20 x 20 inch low turbulence tunnel. This wind tunnel is designed to have free stream turbulence level of only 0.03 per cent. The air velocity was adjustable by speed control of the blower motors in the range from 5 to 30 meters per second. The free stream velocity was measured with a pitot tube and a micro-manometer capable of measuring to within 0.01 millimeters of alcohol. The probe was attached to an arm which projected into the tunnel test section from the bottom, and which could be moved in the direction of the air stream by means of a traversing mechanism; precision turbulence-producing grids could be inserted ahead of the test section if desired. Comparison hot wire anemometer measurements were made with a platinum wire 0.00025 inches in diameter, using an amplifier properly compensated up to ten thousand cycles per second. A 12 inch open jet was also available for low speed measurements in the range from 5 to 30 meters per second. Provision was made for observing the glow through a microscope while it was in this open jet.

The tests in the supersonic speed range were performed in the GALCIT 4 x 10 inch transonic tunnel. The Mach number could be adjusted in the supersonic range from 1.15 to 1.5 by altering the jack settings on the flexible throat. This tunnel is calibrated in such a way that the free stream Mach number can be obtained directly from these jack settings with a precision of about one per cent. A Schlieren system

was available, and enabled shock wave photographs to be taken; it also allowed the Mach number to be checked by measurements of the Mach angle. The probe was attached to an arm which projects from the top of the tunnel test section and which could be moved both in the direction of the air stream, and perpendicular to the air stream by means of a traversing mechanism. Provision was made for observing the glow through a telescope while it was in the test section. Figure (10) shows the probe in position in the test section.

The most important single detail in these experiments was the probe into which the electrodes were built. Figures (11) and (12) are double scale sketches of two typical probes used in the low speed and in the supersonic tests respectively. A number of other slightly modified probes were used. For example, different electrode surface areas were used, the anode area was tried both smaller and larger than the cathode area, and the anode was offset very slightly downstream and upstream of the cathode. These changes did not affect the shape of the calibration curves in any significant manner. These probes are about the same size as standard hot wire anemometer probes, and are considerably stronger. For the probe used at supersonic speeds, a thin (0.01 inches) sheet of platinum was arc-welded to the ends of the projecting steel arms and was ground to the proper size. This allowed the arms to have the strength of steel and still provided the necessary platinum electrode surface. The electrode spacings were measured with a Bausch and Lomb optical comparator capable of a precision of about 0.0001 inches. The spacings were measured with the probe in still air; in the supersonic tests the spacings were considerably decreased by the aerodynamic forces when the

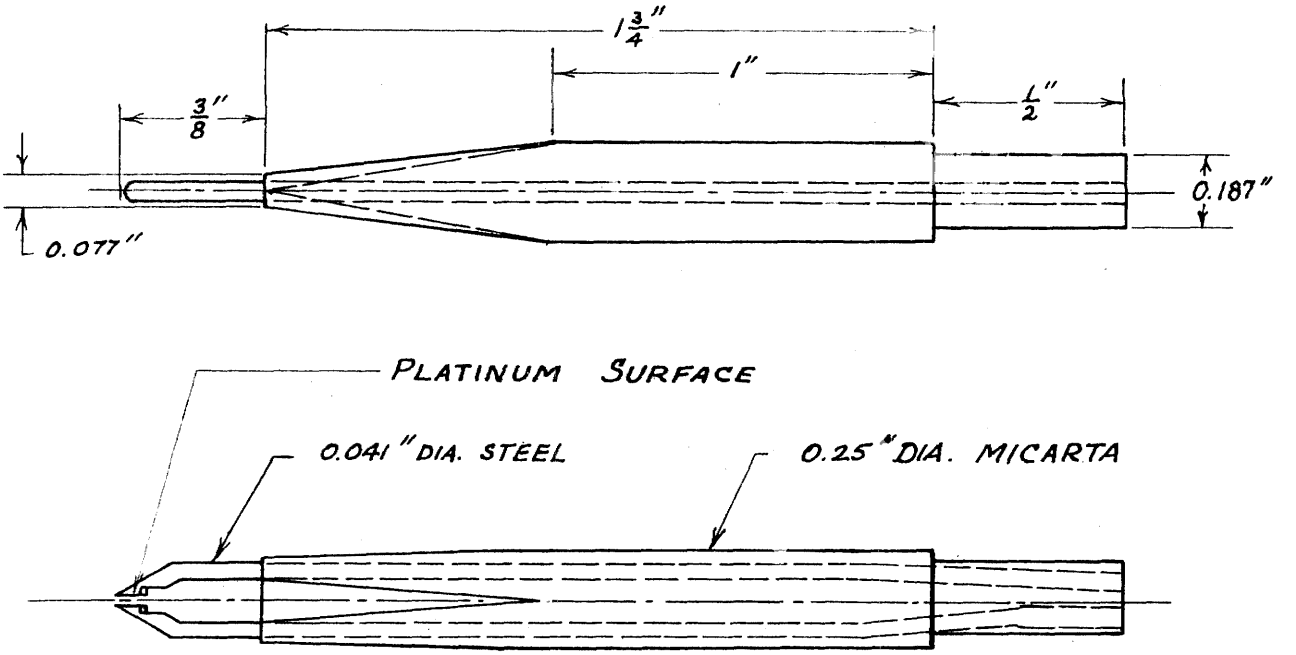


HIGH SPEED PROBE ~ DOUBLE SIZE

FIGURE (12)

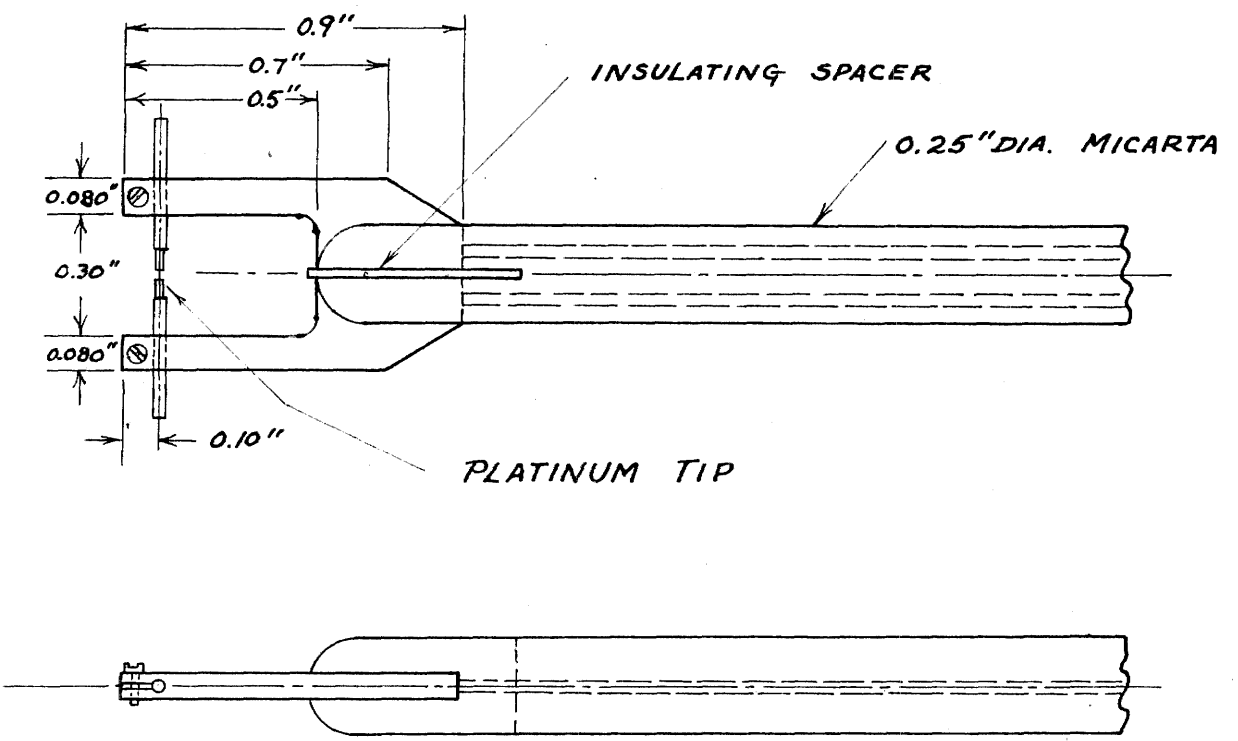


LOW SPEED PROBE ~ DOUBLE SIZE

FIGURE (11)

probe was placed in the air stream. Trial and error adjustments and careful polishing while observing the probe through a microscope were necessary to set the spacing and to get the electrode surfaces exactly flat and parallel (at zero air velocity) with sharp edges. One might logically question the desirability of sharp edges and exact parallelism. However, rigidly adhering to these conditions appeared to be the only way in which a given electrode configuration could be exactly controlled and reproduced in studying the effect of spacing and electrode area. In the final design as an instrument which is calibrated before each use, one would probably round the edges off, and might deliberately avoid exact parallelism.

A variety of anode and cathode materials were tried in order to investigate the possibility that there might be some combination of materials with which the glow could operate with minimum sputtering or maximum stability or both. The following materials of ordinary commercial purity were tried: aluminum, iron, copper, tungsten, platinum, tantalum, duraluminum, and elkonite. Of these materials, only platinum allowed the glow to operate with a low enough noise level and with sufficient stability at atmospheric pressure. However, examining the electrodes under a microscope after operation indicated that platinum sputtered as much or more than any of the other materials. Since the processes important to the glow discharges stability occur in the cathode drop region, one would expect the choice of cathode material to have a greater effect on the stability than the choice of anode material. This was found to be true, and no significant change in stability was noted with a platinum cathode when the anode material was changed from

platinum to tungsten or tantalum. The fact that electrodes of aluminum and tantalum, which are known to operate with much less sputtering than platinum at low pressures, are unsatisfactory from a stability viewpoint suggests that some sputtering might be inherent in a stable glow discharge at atmospheric pressure. It is possible some of the materials which were unsatisfactory might prove useful in either a purer form, or with the proper deliberately added impurities.

The meter used for measuring the direct current voltage across the glow discharge had to be protected, since the voltage across the glow would rise from the operating voltage of about 350 volts to two or three thousand volts (depending upon the specific variac and current regulator settings) if the glow discharge were to suddenly become unstable and be extinguished. This protection was accomplished (see Figure (8)) by putting in parallel with the meter a series of glow tubes selected to have a striking voltage higher than the expected operating voltage of the anemometer but low enough so that the meter would not be damaged if the anemometer were extinguished. Of course, the switch in series with the protective tubes had to be opened when the glow discharge was initially being established.

## IV. EXPERIMENTAL RESULTS

The experimental observations made in connection with this research will now be presented. Many of the experiments were repeated a number of times. In such cases, the data of a representative run are given. It will be observed that much of the data has a considerable scatter and that many points will have to be clarified before the glow discharge anemometer is a finished or even a useful instrument. At several points in the course of this work there was the choice of concentrating on the improvement of a given characteristic or of leaving that characteristic in a somewhat incomplete state and proceeding with an exploration of additional properties and characteristics. The latter course was chosen, since it was felt that this research should provide a general foundation upon which the development of the glow discharge anemometer as a working instrument could be based.

### A. Zero Velocity Data

The first matter which required investigation was the stability of a glow discharge at atmospheric pressure. Platinum electrodes were used. Figure (13) shows the results of a typical run made with the current at five milliamperes and with an electrode spacing of 0.0071 inches. The voltage was recorded every thirty seconds for an hour and fifteen minutes after the glow was established between freshly polished electrodes. It will be observed that after a ten minute warm-up period the maximum deviation from the mean voltage of 355.5 over a period of slightly more than an hour was only about one part in 600. In order to achieve this degree of stability, the current had to be adjusted to a low enough value to prevent the cathode glow from extending over the edges of the cathode. With the electrode configuration used in taking

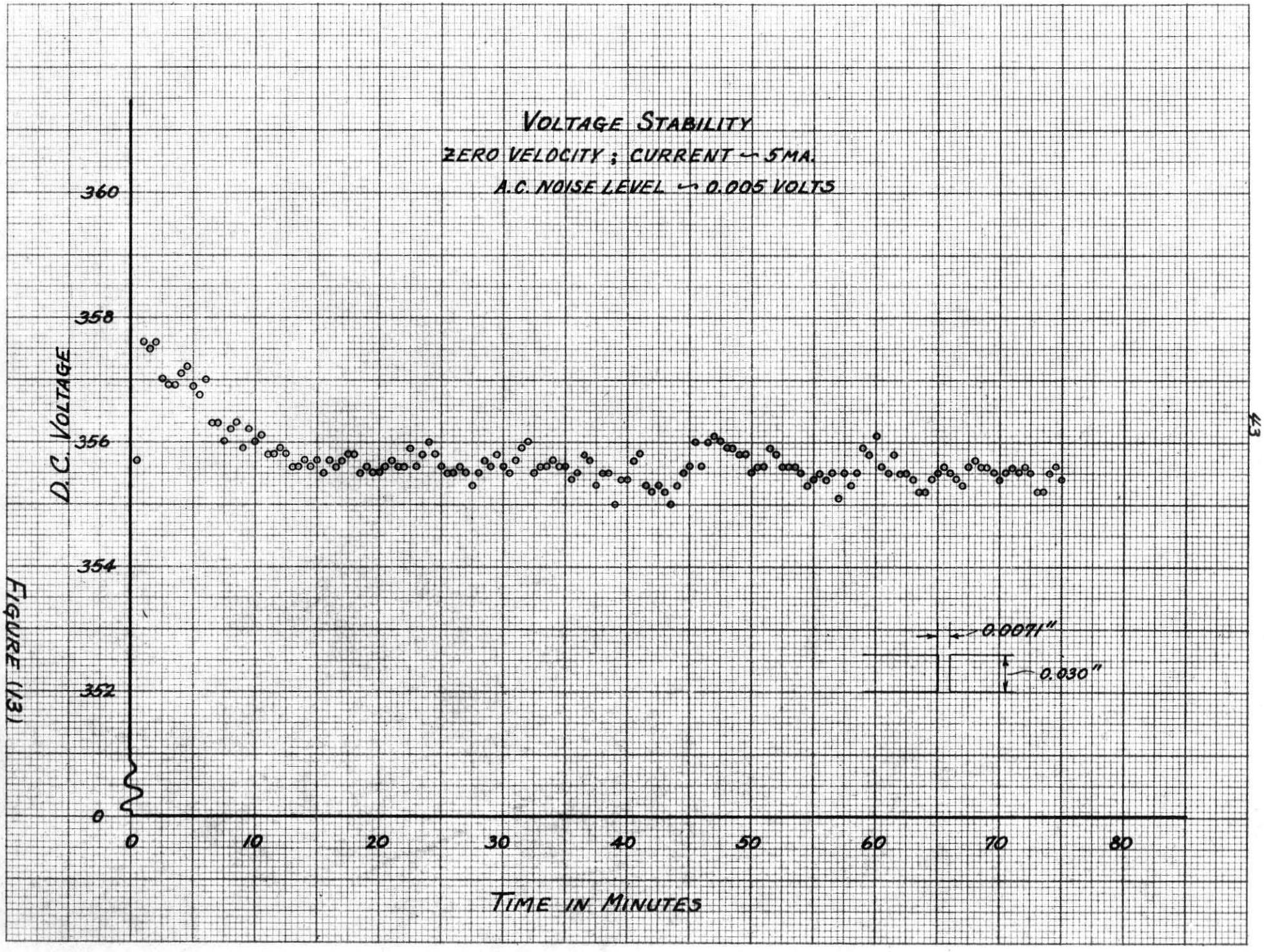
VOLTAGE STABILITY
ZERO VELOCITY ; CURRENT ~ 5 MA.
A.C. NOISE LEVEL ~ 0.005 VOLTS
D.C. VOLTAGE
360
358
356
354
352
0
0
10
20
30
40
50
60
70
80
TIME IN MINUTES
0.0071"
0.030"

FIGURE (13)

the data discussed above, the cathode glow appeared to cover the cathode at a current of 8.5 milliamperes. The deviations about the mean voltage after the first ten minutes are presumably the effects of sputtering, local disturbances on the electrodes caused by minute impurities in the electrodes, and local air currents set in motion by convection. Apparently about ten minutes of operation are required to "condition" the electrodes and to reach temperature equilibrium. This "conditioning" time was consistently observed when first establishing the glow with newly polished electrodes, even though the electrodes were carefully cleaned to remove grease and dirt. Examination of the electrodes under a microscope after sustained operation revealed a shallow crater in the surface of the cathode and a corresponding mound of deposited material on the anode. At spacings below about 0.0035 inches, this mound of material on the anode caused the discharge to short itself after about one-half an hour of operation. (This did not occur when operated in an air stream because the particles transferred from the cathode were practically all carried downstream with the air.)

The effect of pressure on the direct current voltage at constant current and at zero velocity was investigated by simply operating the glow discharge inside a small pressure chamber and recording the voltage as the pressure was varied. These data are presented by Figure (14). It became more difficult to establish a stable glow as the pressure was increased. An increase in air pressure from atmospheric pressure to 45 pounds per square inch caused a voltage increase of 17.5 volts. When operating the glow discharge in a moving air stream, an increase in velocity was accompanied by a voltage increase and by a decrease in the pressure between the electrodes. Therefore, in view of

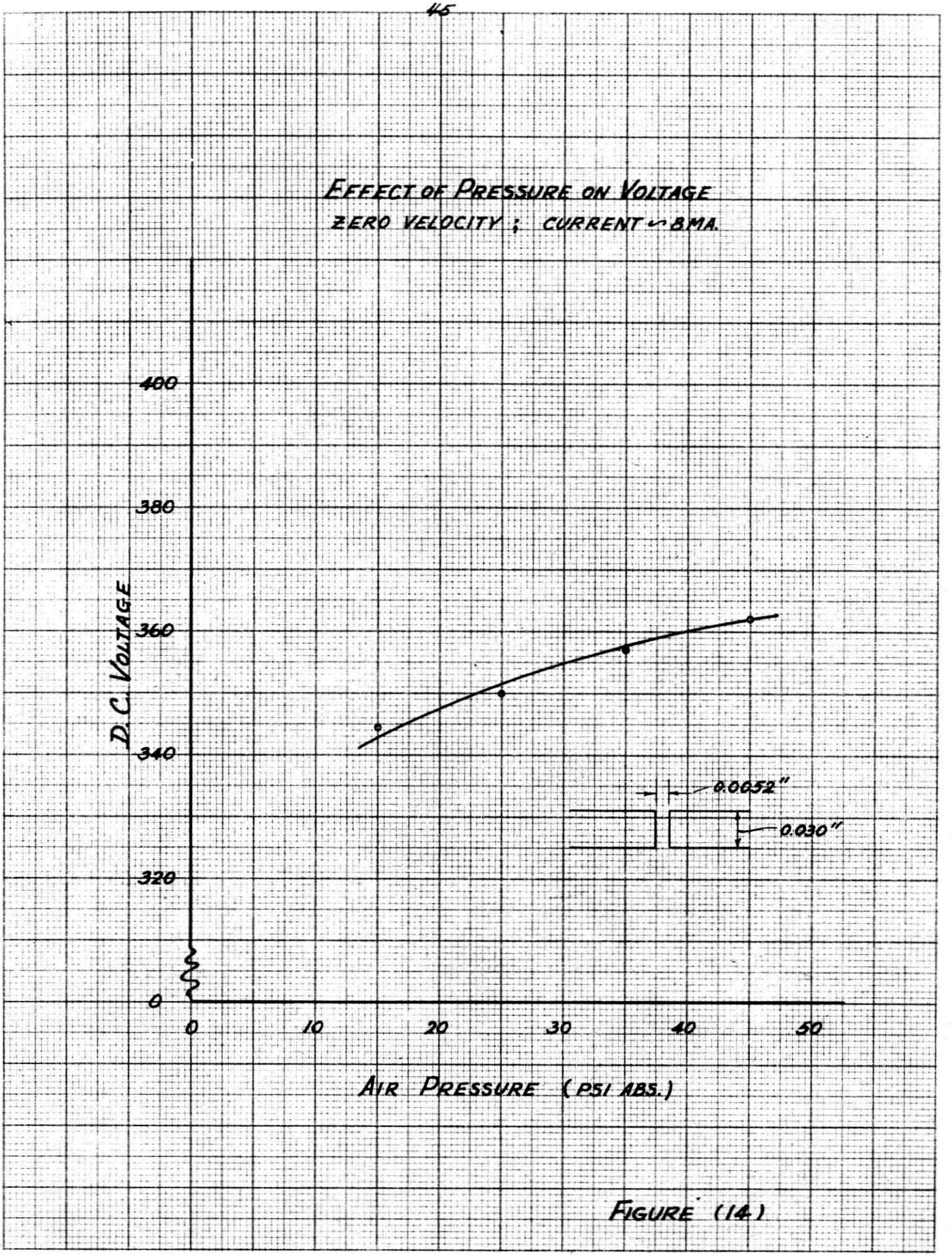
EFFECT OF PRESSURE ON VOLTAGE
ZERO VELOCITY ; CURRENT ~ 8 MA.
D.C. VOLTAGE
400
380
360
340
320
0
0
10
20
30
40
50
AIR PRESSURE (PSI ABS.)
0.0052"
0.030"

FIGURE (14)

Figure (14), the pressure effects cannot account for the increase of voltage with increasing velocity. Furthermore, at low subsonic velocities, the changes in pressure will be considerably less than one pound per square inch, and the "negative" pressure effects will not be significant. No data were taken at pressures less than atmospheric; however, since the mean free path depends inversely on pressure, one would expect that the voltage would change about as much between 15 and 7.5 pounds per square inch as it did between 30 and 15 pounds per square inch.

The effect of ambient temperature on the voltage across the glow was determined by placing the probe in an oven and allowing it to reach temperature equilibrium, and then establishing the glow and recording the voltage as a function of time as the new temperature equilibrium was reached. These data are plotted in Figure (15); the probe was of the type shown in Figure (11) and the spacing was 0.0060 inches. The glow was operated for about 10 minutes to "condition" the electrodes before the first run. The voltage changes are presumably caused by expansion of the electrodes and the electrode supports and will, therefore, depend upon the particular construction of the probe used; the effect of ambient temperature changes of a few hundred degrees Fahrenheit on the atomic properties of the air is considered to have only a negligible effect on the voltage. The rather interesting behavior during the first minute after the glow was established is believed to be due to a combination of the effects of local convection currents and local expansions as part of the heat produced by the glow is conducted along the electrodes to the supports, causing a new temperature equilibrium to be reached. When operating the glow discharge in an air stream a

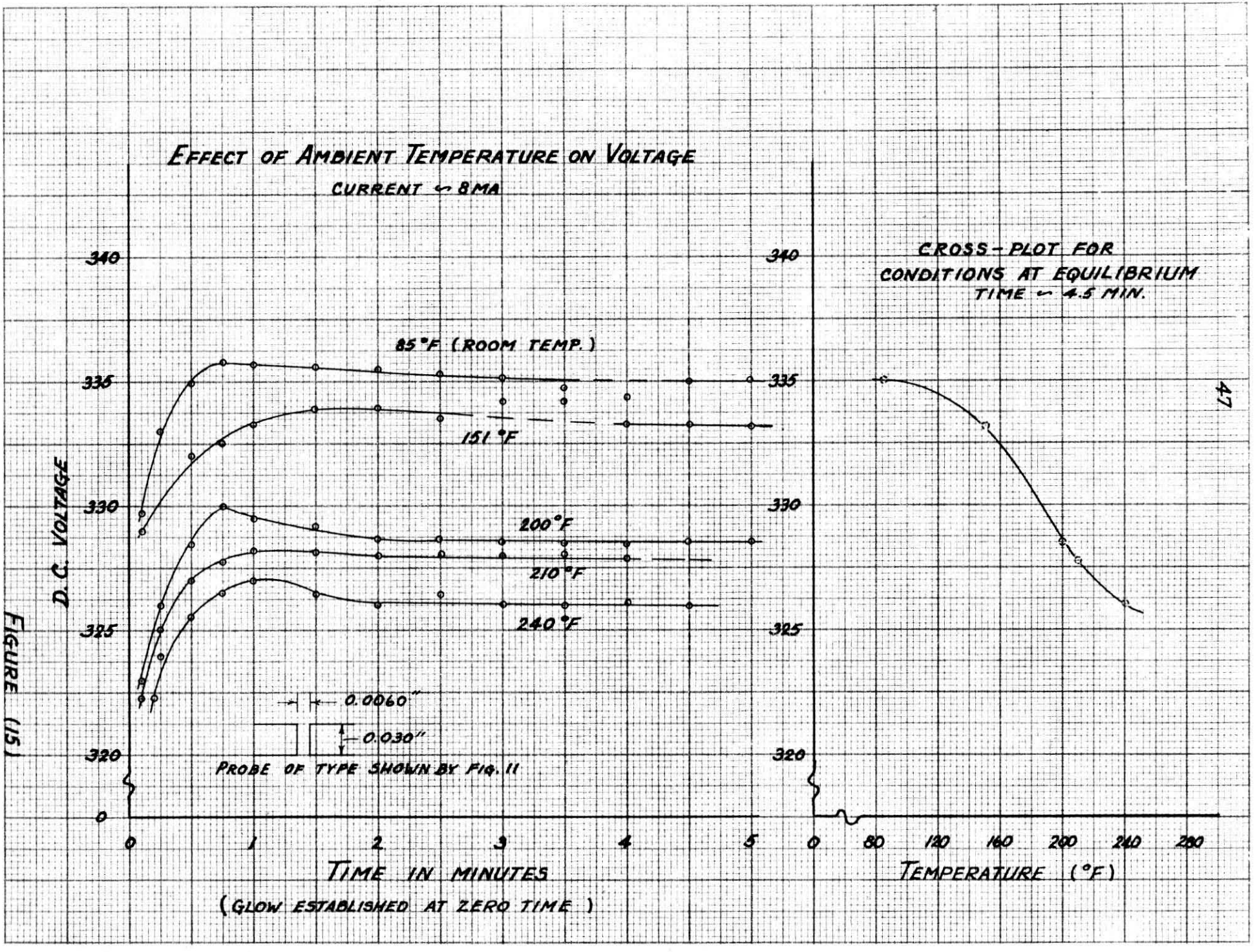
EFFECT OF AMBIENT TEMPERATURE ON VOLTAGE
CURRENT ~ 8 MA
85 °F (ROOM TEMP.)
151 °F
200 °F
210 °F
240 °F
D.C. VOLTAGE
340
335
330
325
320
0
0.0060"
0.030"
PROBE OF TYPE SHOWN BY FIG. 11
0
1
2
3
4
5
TIME IN MINUTES
(GLOW ESTABLISHED AT ZERO TIME)
CROSS-PLOT FOR
CONDITIONS AT EQUILIBRIUM
TIME ~ 4.5 MIN.
0
80
120
160
200
240
280
TEMPERATURE (°F)

FIGURE (15)

large portion of the heat produced by the glow is carried downstream, and the heat transfer from the probe is increased as the velocity increases. The temperature of the probe therefore decreases. However, the probe temperature probably does not change more than twenty or thirty degrees Fahrenheit as the velocity is increased from a few meters per second to fifty or sixty meters per second. Comparison of Figures (15) and (18) will thus reveal that only a small part of the observed voltage change is due to the spacing changes caused by temperature effects. Furthermore, since it requires several minutes to reach temperature equilibrium, rapid velocity fluctuations such as turbulence will cause no appreciable change in spacing.

B. Subsonic Velocity Data

As indicated in the section describing the apparatus used, a preliminary survey was first made to roughly determine the velocity and current ranges through which a stable glow discharge could be maintained. In this early work, the spacings were not measured with the optical comparator later used, but were estimated by means of a feeler gauge. Also, the velocities could not be measured directly; instead the pressure and temperature just ahead of the nozzle (which exhausted to the atmosphere) were read. These approximate data are presented in Figure (16) and (17). It will be observed that as the velocity was increased, the current necessary for stable operation likewise increased. It should be noted that the glow discharge was essentially operating in an open jet, and was therefore at approximately atmospheric pressure. The electrodes used here had a smaller surface area than those used in the more precise tests made later; observation under a microscope showed that the cathode

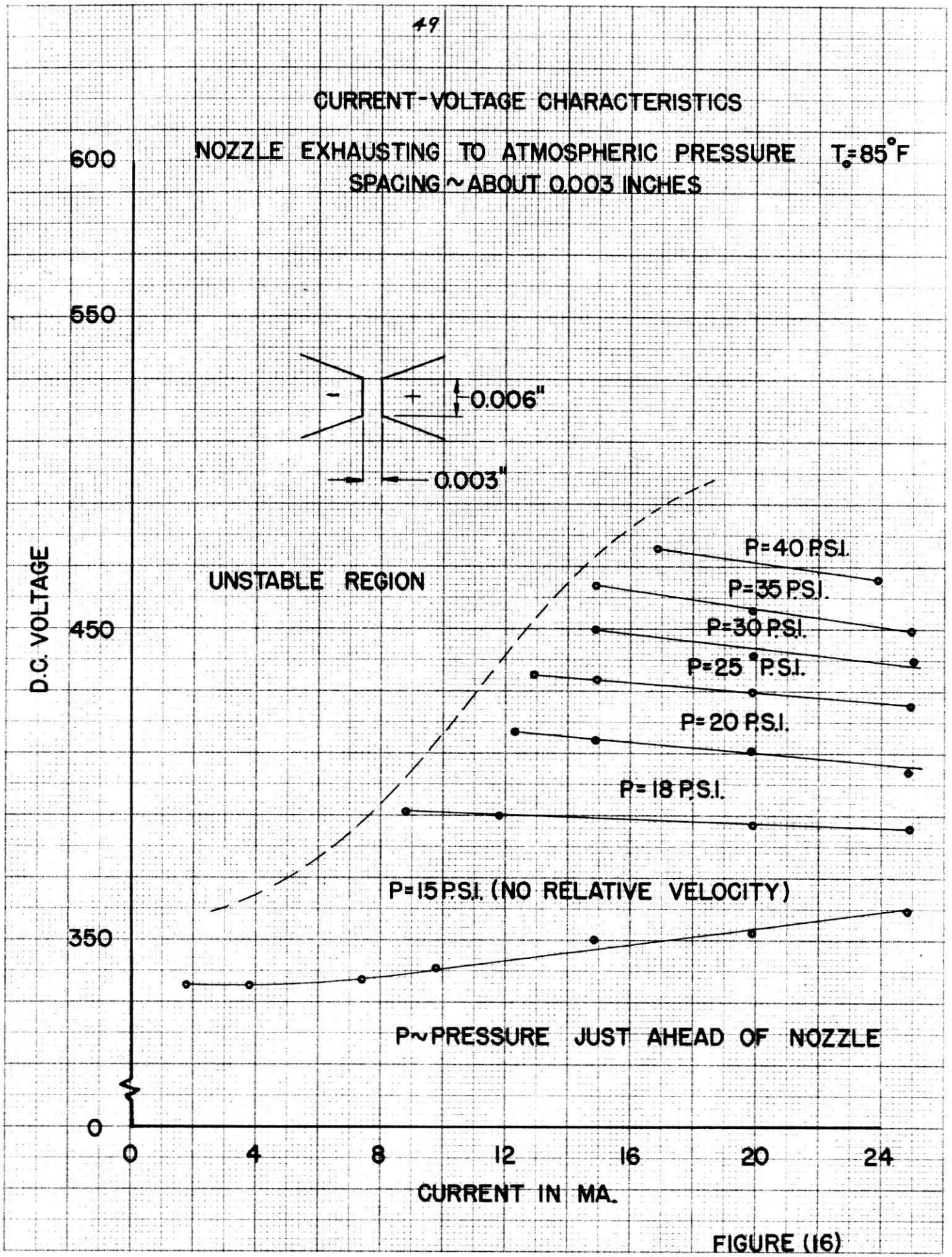
CURRENT-VOLTAGE CHARACTERISTICS
NOZZLE EXHAUSTING TO ATMOSPHERIC PRESSURE T=85°F
SPACING ~ ABOUT 0.003 INCHES
600
550
450
350
0
D.C. VOLTAGE
-
+
0.006"
0.003"
UNSTABLE REGION
P=40 P.S.I.
P=35 P.S.I.
P=30 P.S.I.
P=25 P.S.I.
P=20 P.S.I.
P=18 P.S.I.
P=15 P.S.I. (NO RELATIVE VELOCITY)
P~PRESSURE JUST AHEAD OF NOZZLE
0
4
8
12
16
20
24
CURRENT IN MA.

FIGURE (16)

# CURRENT–VOLTAGE CHARACTERISTICS

NOZZLE EXHAUSTING TO ATMOSPHERIC PRESSURE

SPACING : ABOUT 0.004 INCHES $T_o \sim 88°F$

P ~ PRESSURE JUST AHEAD OF NOZZLE

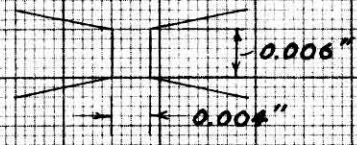


P ~ 45 PSI.

P ~ 35 PSI.

REGION OF INSTABILITY

P ~ 30 PSI.

P ~ 25 PSI.

P ~ 20 PSI.

P ~ 15 PSI. (NO AIR FLOW)

D.C. VOLTAGE

650
600
500
400
300
0

0 5 10 15 20 25

CURRENT IN MA.

FIGURE (17)

glow extended around the edges of the cathode for currents greater than about seven milliamperes. Although using the pressure data taken, one could calculate the velocity in throat of the nozzle in the absence of the electrodes with reasonable accuracy, it is difficult to estimate the velocity at the throat with the electrodes inserted through the walls of the throat. However it appears reasonable that as the pressure ahead of the nozzle reaches about 35 pounds per square inch, the velocity at the electrodes is of the order of 350 meters per second. One thus concludes that a stable glow discharge can be maintained throughout the range from zero velocity to high subsonic velocities. This result warranted a more careful study of the properties of a glow discharge in an air stream.

After the preliminary survey described above, the glow discharge was operated in the 12 inch open jet and in the low speed wind tunnel previously described. The object of the tests performed was to determine whether or not the glow discharge could be used to obtain quantitative measurements of turbulence at low air speeds. Specifically the decay of turbulence behind a one-inch grid was measured and compared with independent measurements made with a hot wire anemometer. Before discussing the results of this decay study, the problems encountered in calibrating the glow discharge anemometer will be considered.

A considerable amount of time was spent in trying different probe configurations and different cathode areas, and in learning how to get the electrodes parallel, how to polish the electrodes, and how to set the spacings. Observation of the glow (with cathode and anode diameters of 0.030 inches) under a microscope while the air velocity was being varied revealed that whereas the cathode glow appeared to move

uniformly downstream as the velocity was increased, the anode glow appeared to move in jerks. By decreasing the size of the anode to 0.010 inches in diameter the anode spot was restricted to one location, and the scatter in the data was somewhat reduced. For best operation, the current was adjusted to allow the cathode glow to cover the cathode area at zero velocity. As the velocity was increased, stable operation was possible until about one quarter of the cathode glow had moved around the downstream edge of the cathode. Further velocity increases then caused instability.

A typical set of calibration curves is shown in Figure (18); each point was taken under equilibrium conditions. These characteristics were intended to be used in the following way; the inverse of the slope of the curve of voltage versus velocity is $\frac{\Delta U}{\Delta V}$ ; at any mean velocity $U$ , measured alternating voltages caused by turbulence can be converted to alternating velocities by multiplying by $\frac{\Delta U}{\Delta V}$ , provided that such alternating voltages are so small that the curve is essentially linear in the range traversed. This calibration procedure assumes that at the frequencies considered, the curve taken under equilibrium conditions will also represent the dynamic response. (See previous discussion on Page 33 .) It will be observed that by properly selecting the spacing, several sensitivities are available in any particular velocity range; the linear portions of the curves would presumably be used whenever possible. The curve given in Figure (18) for a spacing of 0.0067 inches shows a definite deviation from the general trend of the curve in the vicinity of 14 meters per second. Such behavior was not characteristic of any particular spacing or of any particular velocity range. Not all sets of calibration curves showed such an anomaly.

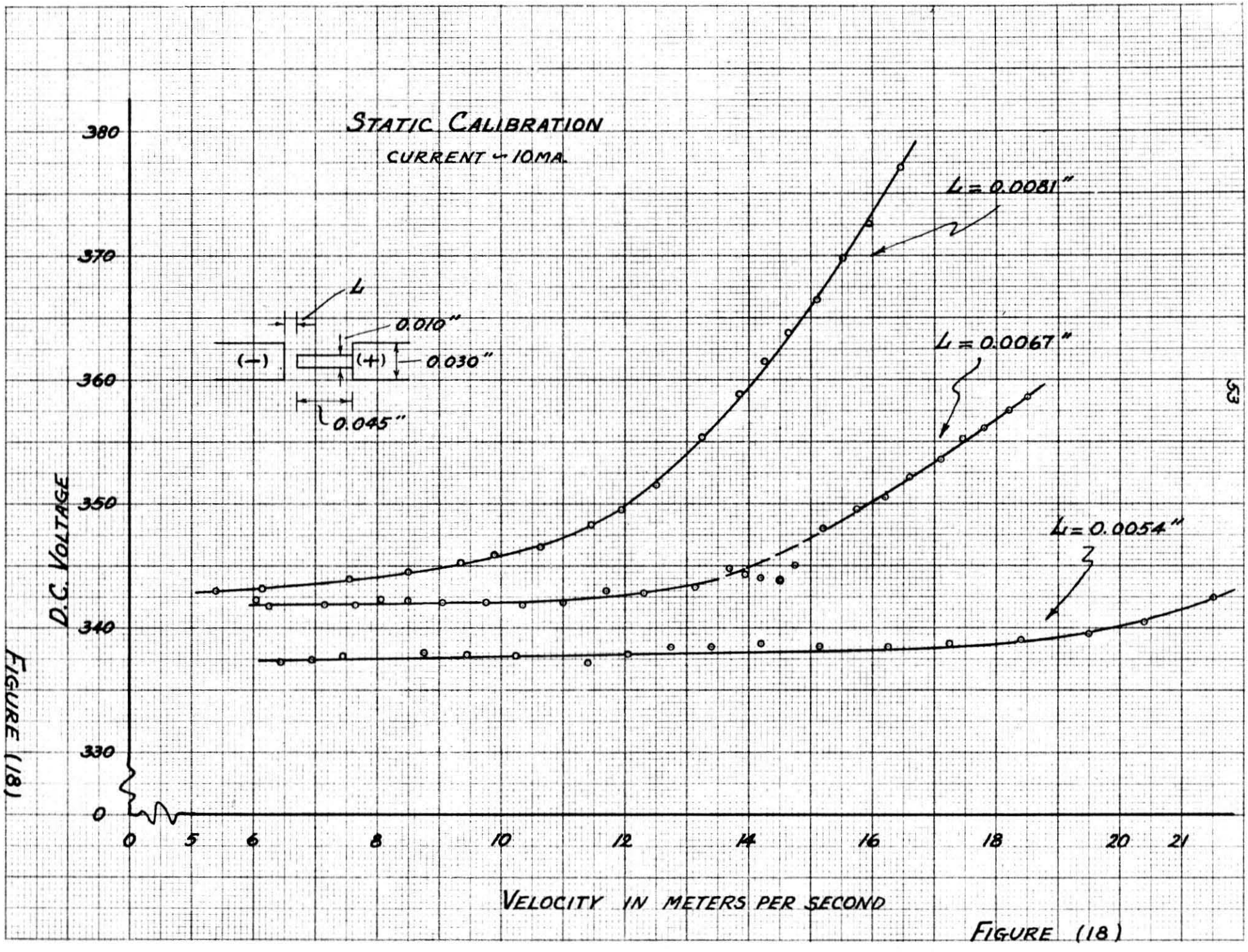


FIGURE (18)

FIGURE (18)

However, since such behavior could not be predicted, and was never entirely eliminated, a set of calibration curves illustrating such behavior is presented in preference to a smooth set.

Curves taken at other values of current are similar in their dependence upon spacing. However, at a given spacing, decreased current causes the voltage to increase more rapidly with velocity and raises the level of the entire curve. This is illustrated by Figure (19).

It took about an hour to take the data for one velocity characteristic such as those shown in Figure (18), since at each point the glow was allowed to operate for several minutes to insure the attainment of equilibrium conditions. If the voltage was then again recorded as the velocity was slowly reduced, it was found that the curve did not exactly retrace itself; the amount by which the curves failed to retrace themselves increased if the current was increased. This pseudo-hysteresis effect was attributed to sputtering of the electrodes, and is illustrated by Figure (20), where the upper curve of Figure (18) is re-plotted, and the points taken as the velocity was slowly decreased are included. It will be observed that the direct current voltage level of the curve is raised about one part in one hundred by sputtering; the slope in the linear portion of the curve is not changed a great amount.

For turbulence measurements at a given mean velocity it is only necessary to know the slope of the calibration curve in the vicinity of that mean velocity. Since the deviations from the mean velocity caused by turbulence at low velocities are generally less than one meter per second, three or four points in the vicinity of the mean velocity are sufficient to establish the required slope of the voltage-velocity

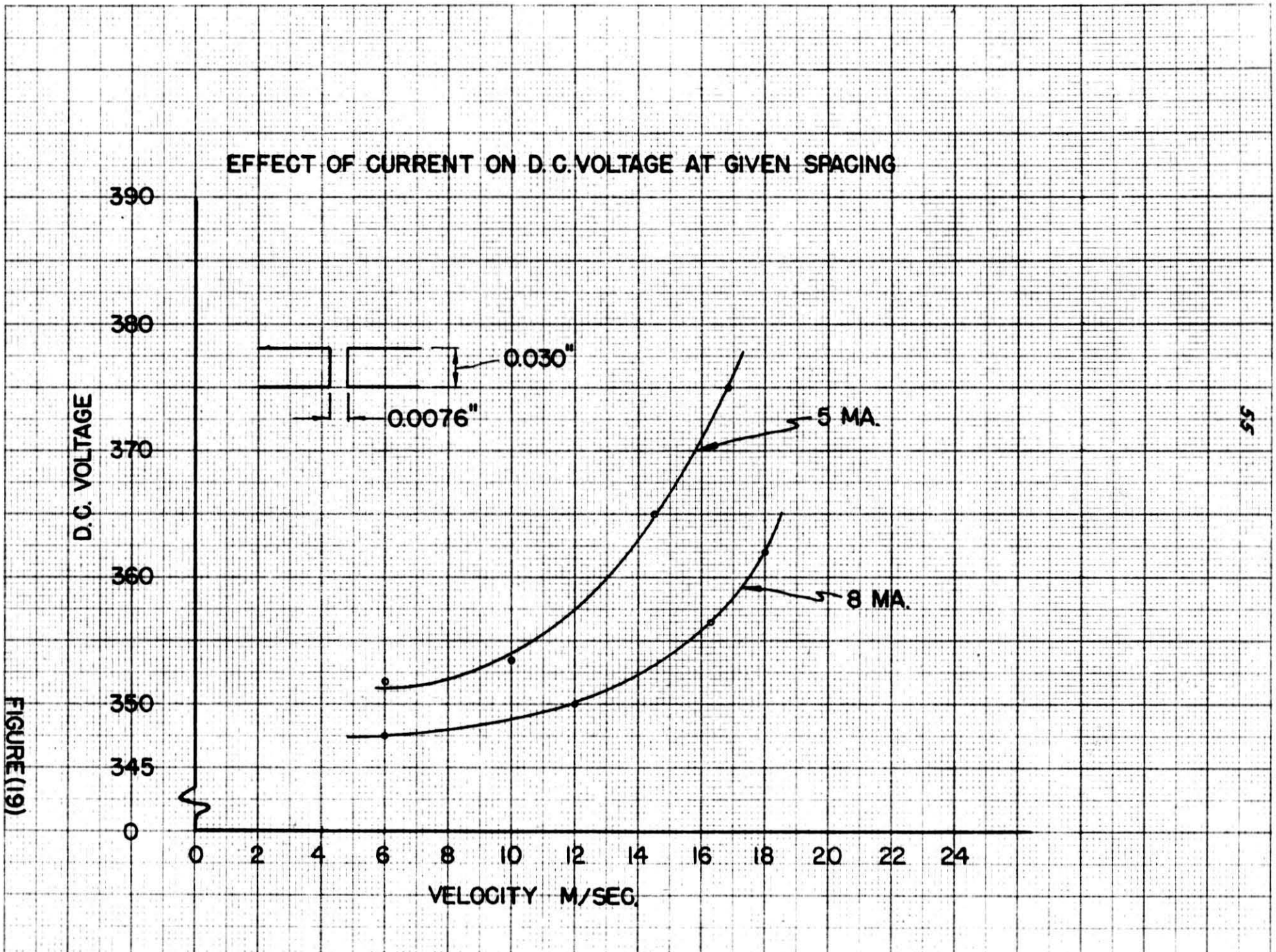
EFFECT OF CURRENT ON D.C. VOLTAGE AT GIVEN SPACING
D.C. VOLTAGE
390
380
370
360
350
345
0
0.030"
0.0076"
5 MA.
8 MA.
0
2
4
6
8
10
12
14
16
18
20
22
24
VELOCITY M/SEC.

FIGURE (19)

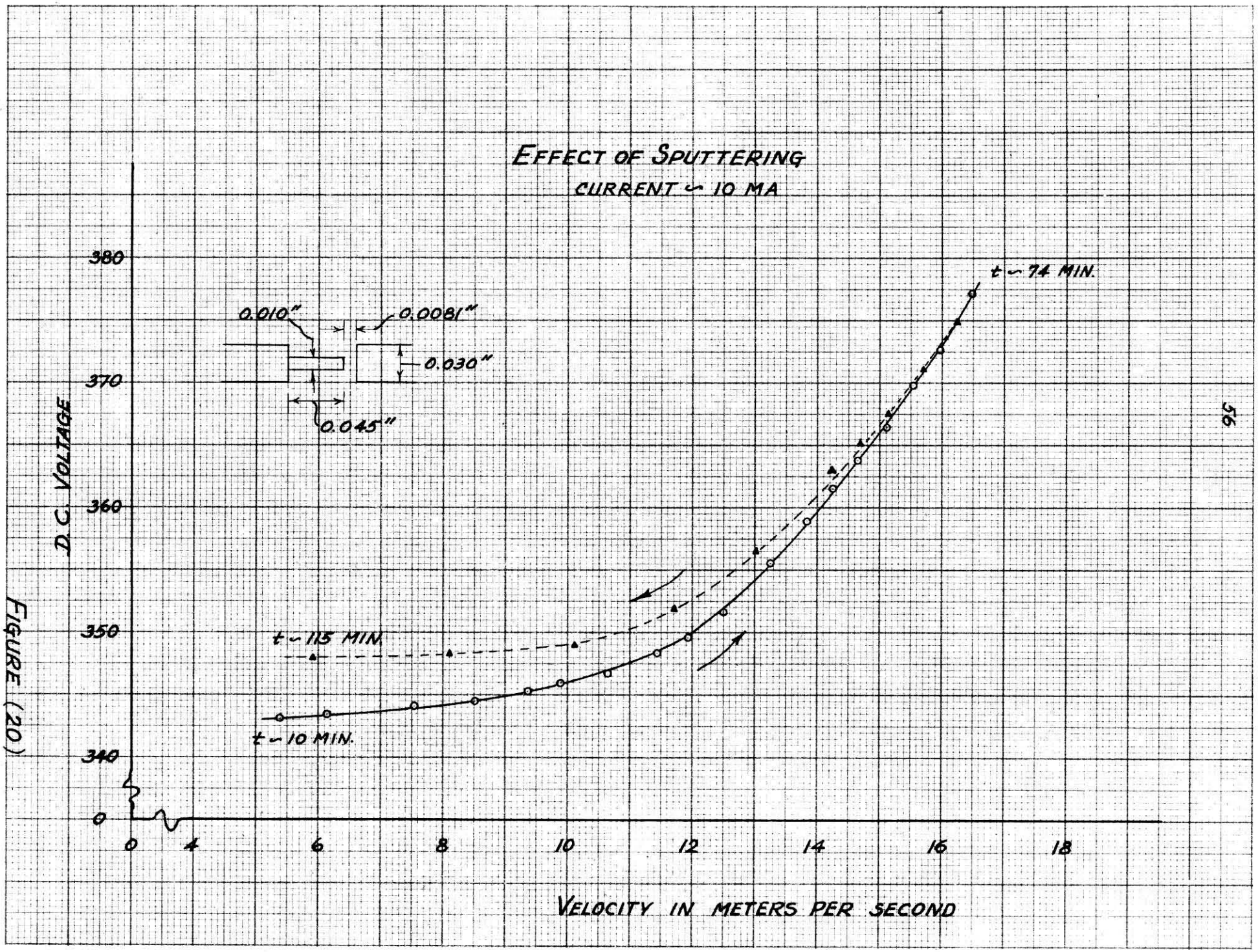


FIGURE (20)

characteristic. One can thus use characteristics such as those shown on Figure (18) to select the spacing necessary to give the desired sensitivity and linearity at the mean velocity under consideration. The actual calibration can then be quickly made just before the alternating "turbulence voltages" are measured by taking just enough points to establish the slope of the characteristic at the mean velocity under consideration. After about twenty minutes of operation, a quick re-calibration can be made.

In measuring turbulence behind a grid, it appeared that since the turbulence level might affect the calibration, the calibrating points should be taken under the actual conditions of measurement, i.e. with the grid in the tunnel, rather than in "turbulence-free" flow. Two calibration curves taken immediately following each other with and without the screen in the tunnel (all other conditions being identical) are presented in Figure (21). It will be observed that the presence of the screen (i.e. the increased turbulence level) shifted the curve upward without greatly affecting the sensitivity (slope). A more detailed presentation of the effect of the turbulence level on the direct current voltage is presented by Figure (22). The values of turbulence level were determined with a hot wire anemometer.

From the above discussion of calibration, one concludes that although both the turbulence level and the electrode sputtering affect the direct current voltage level of the calibration curves, they do not greatly affect the slope of the curves. Hence, although the necessity of repeated calibrations complicates the operating technique of the glow discharge anemometer, the calibration procedure outlined above appears adequate; it could probably be considerably refined. A set of calibration

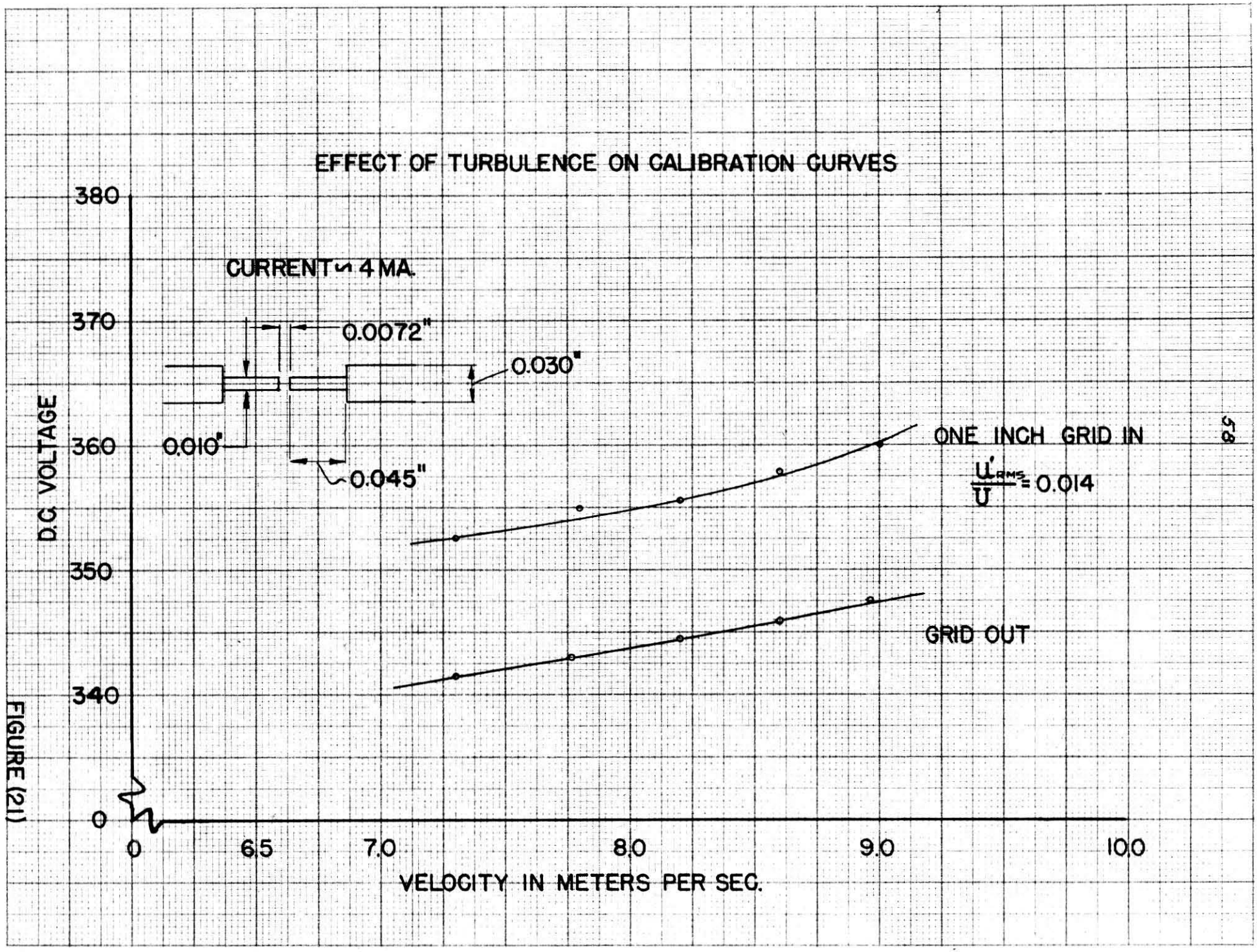
EFFECT OF TURBULENCE ON CALIBRATION CURVES
380
370
360
350
340
0
D.C VOLTAGE
CURRENT ~ 4 MA.
0.0072"
0.030"
0.010"
0.045"
ONE INCH GRID IN
$\frac{U'_{RMS}}{U}$ = 0.014
GRID OUT
0
6.5
7.0
8.0
9.0
10.0
VELOCITY IN METERS PER SEC.

FIGURE (21)

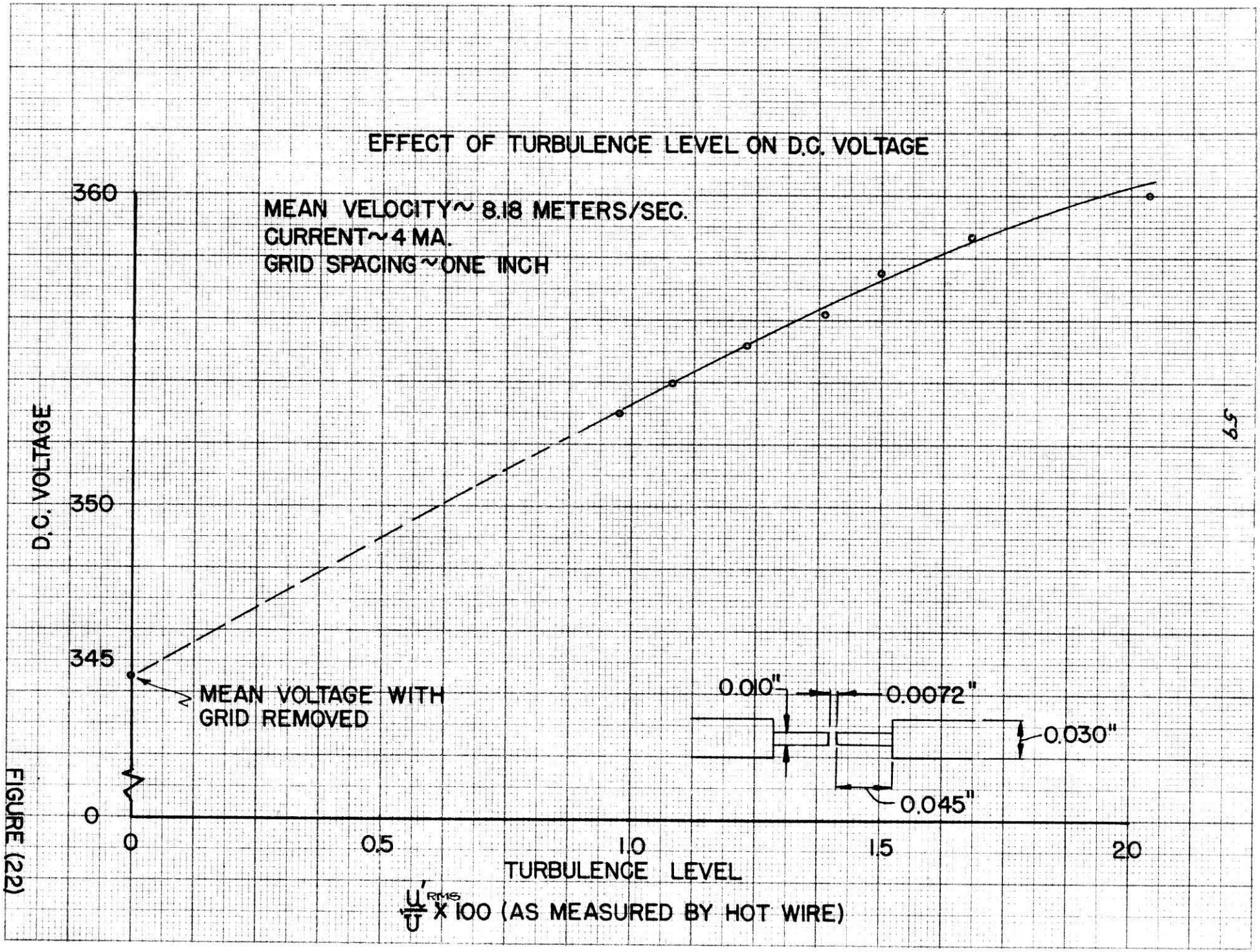
EFFECT OF TURBULENCE LEVEL ON D.C. VOLTAGE
MEAN VELOCITY~ 8.18 METERS/SEC.
CURRENT~4 MA.
GRID SPACING~ONE INCH
D.C. VOLTAGE
360
350
345
0
MEAN VOLTAGE WITH GRID REMOVED
0.010"
0.0072"
0.030"
0.045"
0
0.5
1.0
1.5
2.0
TURBULENCE LEVEL
$\frac{U'_{RMS}}{U} \times 100$ (AS MEASURED BY HOT WIRE)

FIGURE (22)

curves taken at intervals of about one-half hour during the course of several runs at a mean velocity of 11.3 meters per second is illustrated as Figure (23). These calibration curves are the ones which were used in obtaining the data discussed in the following paragraph.

In measuring the decay of turbulence behind a one inch screen, the root mean square of the alternating component of voltage across the glow (of the order of one volt) was measured as a function of the distance from the screen which produced the turbulence. Using the calibration curves given in Figure (23), the values of $\frac{u'_{RMS}}{U}$ were calculated. The quantity $\frac{u'_{RMS}}{U}$ was also determined independently by measurements with a hot wire anemometer. A typical set of these data are presented as Figure (24). It will be observed that one run made with the glow discharge anemometer lies in the vicinity of the hot wire anemometer results, while the other run has several points which check nicely, but then deviates completely from the hot wire results. The calibration curves used (see Figure (23)) were taken at the beginning of the first run, and at the beginning and end of the second run. Several other runs taken resulted in a decay curve which lay above the hot wire results for the entire traverse down the tunnel.

Some light is cast upon the irregular behavior shown in Figure (24) by the film records of the alternating voltage waveforms observed on the oscilloscope while the data was being taken. Figure (25) is a photograph of the type of waveform observed while taking data at a point such as point A of Figure (24). Figure (26) is a photograph of the type of waveform observed at a point such as point B of Figure (24). These photographs were taken with a moving-film camera with a film speed of about 200 feet per minute; the horizontal gain on the oscilloscope was

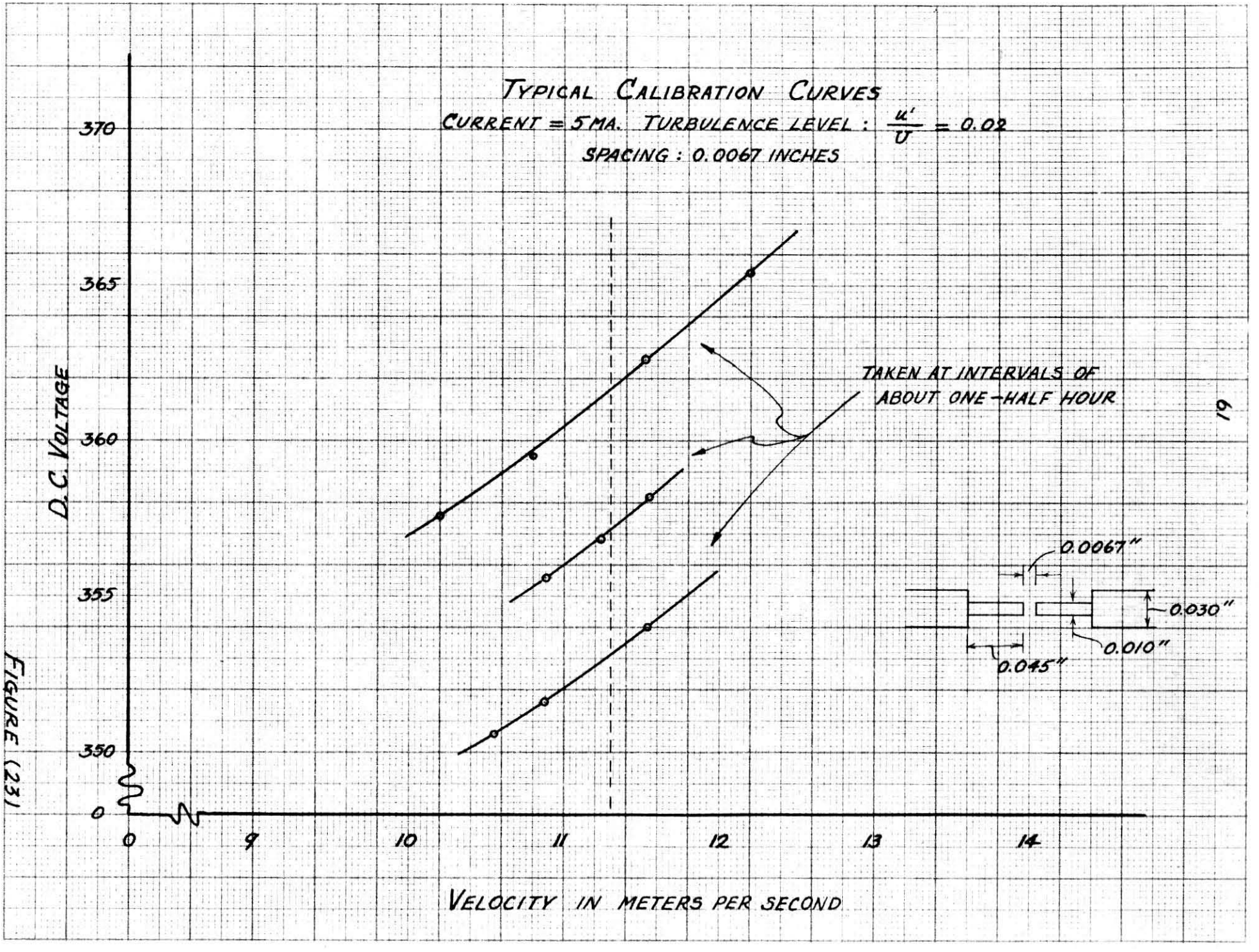
TYPICAL CALIBRATION CURVES
CURRENT = 5 MA. TURBULENCE LEVEL : u'/U = 0.02
SPACING : 0.0067 INCHES
TAKEN AT INTERVALS OF ABOUT ONE-HALF HOUR
D.C. VOLTAGE
370
365
360
355
350
0
0
9
10
11
12
13
14
VELOCITY IN METERS PER SECOND
0.0067"
0.030"
0.010"
0.045"

FIGURE (23)

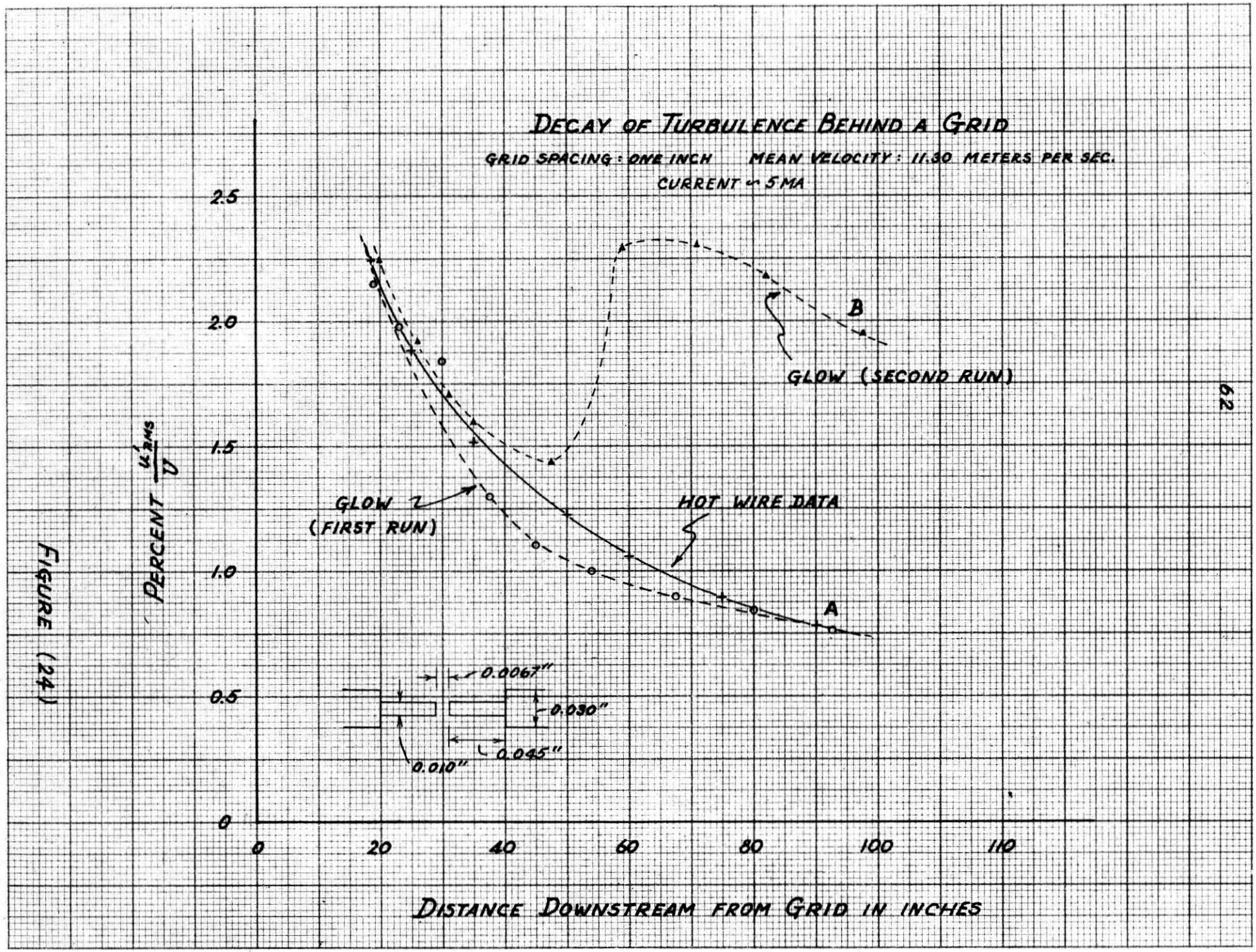
DECAY OF TURBULENCE BEHIND A GRID
GRID SPACING : ONE INCH MEAN VELOCITY : 11.30 METERS PER SEC.
CURRENT = 5 MA
PERCENT $\frac{u'^2_{RMS}}{U}$
2.5
2.0
1.5
1.0
0.5
0
0
20
40
60
80
100
110
B
GLOW (SECOND RUN)
GLOW (FIRST RUN)
HOT WIRE DATA
A
0.0067"
0.030"
0.045"
0.010"
DISTANCE DOWNSTREAM FROM GRID IN INCHES

FIGURE (24)

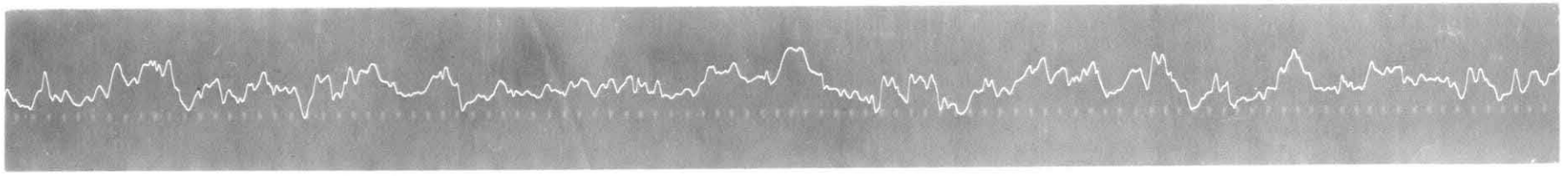

VOLTAGE ACROSS GLOW DISCHARGE WHEN PLACED IN A TURBULENT AIR STREAM

Timing marks: 500 per second

Figure (25)

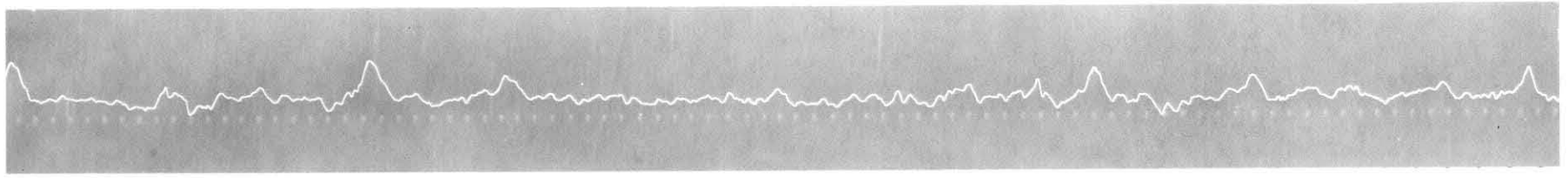

NON-RANDOM FLUCTUATIONS SOMETIMES OBSERVED

Gain reduced to $\frac{1}{2}$ of that used for Figure (25)
Timing marks: 500 per second

Figure (26)

reduced to zero while the pictures were being taken. It will be observed that Figure (25) exhibits the expected random fluctuations of turbulence. On the other hand, the waveform shown by Figure (26) is definitely not random, since the large peaks occurring periodically are all in the same direction. There appear to be several possible explanations for these uni-directional voltage peaks: they may be related to sputtering or loss of material from the electrodes: they may be caused by sudden rapid changes in the sensitivity; or they may be aerodynamic in nature. At the velocity used in taking the data presented as Figure (24), the size of the smallest turbulent eddies is of the order of one millimeter; the spacings used and the electrode dimensions were thus several times smaller than the eddies. The nature of the flow between the electrodes under such conditions is an open question. The uni-directional voltage peaks could conceivably correspond to a sudden instability or change in the flow conditions between the electrodes. Additional study of the discrepancy between the measurements made with the glow discharge anemometer and with the hot wire anemometer is necessary. The noise level associated with the turbulence decay measurements (Figure (24)) is of interest. With the glow operating in still air, the average alternating voltage level was about 0.004 volts; this voltage was not completely steady, and would occasionally rise to several times the average value for a fraction of a second. The alternating voltages read and interpreted as being due to turbulence were of the order of one volt at a turbulence level of about two percent and at a mean velocity of 11.3 meters per second, i.e. about 250 times the average zero velocity noise level.

The free stream turbulence level of the wind tunnel used is about 0.03 per cent as measured by the hot wire anemometer when no turbulence-producing grids are placed ahead of the test section. Since the sensitivity as determined by the calibration curves was not greatly affected by the turbulence level (See Figure (21)) one would expect that the alternating voltage measured at 11.3 meters per second in the open test section (i.e without a grid) would be of the order of 0.015 volts. $\left[\frac{0.03}{2.0} \times 1.0\right]$ . This was not the case. Instead the alternating voltages in the open test section varied from two to twenty times this expected value during the course of several experimental runs. Evidently the glow is either extremely sensitive to low turbulence levels in a manner not predicted by the calibration curves, or the mere presence of the air velocity without any appreciable turbulence introduces a noise voltage far greater than the noise voltage measured at zero velocity. Additional investigation of the noise problem is necessary.

C. Supersonic Velocity Data

The problem of making measurements in a supersonic air stream with a probe-type instrument is complicated by the formation of shock waves ahead of the probe. It is impossible to make direct measurements of free stream conditions by inserting a probe of any kind into a supersonic flow. One can only measure the conditions behind the shock wave formed ahead of the probe. If the strength of the shock wave is known and if the manner in which a shock wave alters the quantity being measured is known, then the free stream conditions can be calculated from the measured data. Since the available information on free stream "turbulence" in a supersonic air stream, and its interaction with a shock wave, is meager at best, its measurement by means of any probe-type

instrument will be quite difficult.

The glow discharge anemometer was tested at supersonic velocities in the GALCIT 4 x 10 inch transonic tunnel. It was found that the glow was stable and could be operated over a wide range of currents. Figure (27) shows a Schlieren photograph taken while the glow was in operation in a supersonic air stream. The photograph shown as Figure (28) was taken at the same Mach number with the glow absent. By superimposing the negatives of these photographs, it was observed that the glow discharge did not affect the shock wave system. These figures show that the shock wave with the probe used is detached and that just ahead of the glow, it is normal to the flow direction. The action of the air stream in forcing the glow to the downstream side of the electrodes is also demonstrated. Careful visual observation of the glow while it was in the air flow revealed a luminous region trailing out of the downstream side of the discharge. This effect was interpreted as being visual evidence of the loss of positive ions out of the discharge.

A typical current-voltage characteristic, taken at a Mach number of about 1.2 is given as Figure (29). The glow was stable at this Mach number at a current as low as six milliamperes and was observed to become more stable as the free stream Mach number was increased. This behavior is different than that observed at high subsonic velocities, where currents of the order of 20 milliamperes were required for stable operation and increasing the velocity made it more difficult to maintain a stable glow. There are two reasons for this difference. At the Mach number and stagnation pressure at which these data were taken, the pressure behind the normal shock wave just ahead of the glow is only about

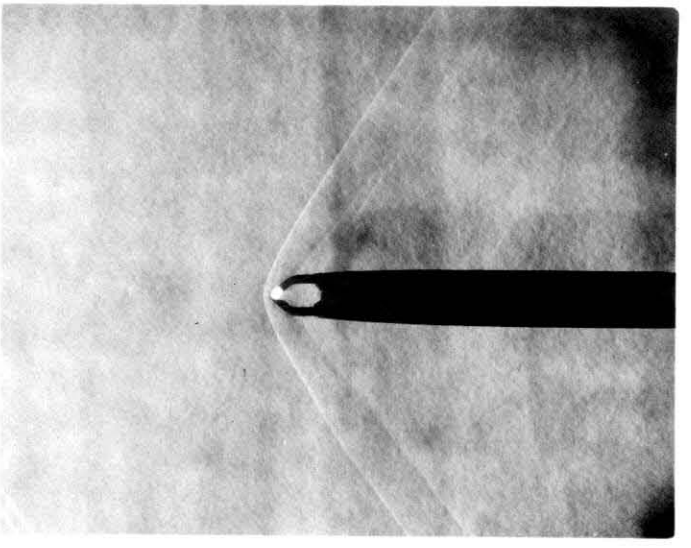

GLOW DISCHARGE ANEMOMETER IN SUPERSONIC AIR STREAM

Mach Number: about 1.2

Figure (27)

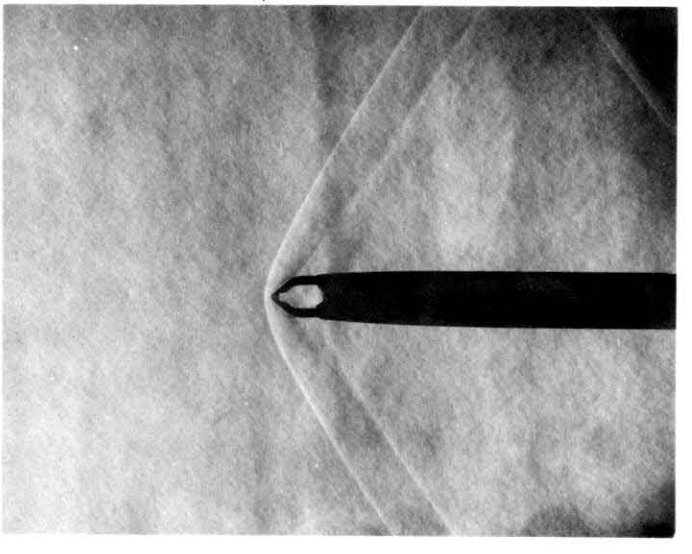

PROBE IN SUPERSONIC AIR STREAM

Mach Number: about 1.2

Figure (28)

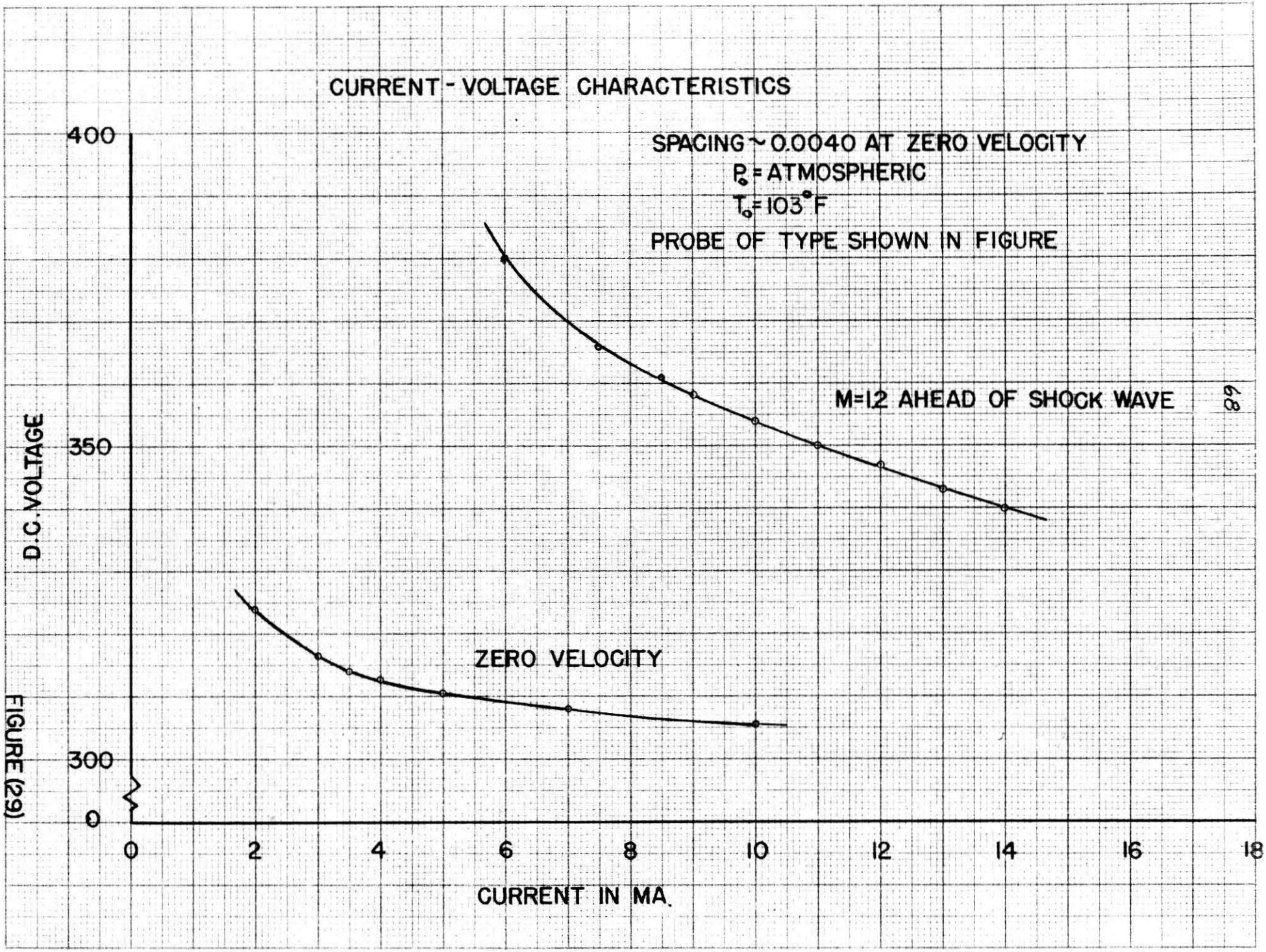
CURRENT - VOLTAGE CHARACTERISTICS
SPACING ~ 0.0040 AT ZERO VELOCITY
$P_o$ = ATMOSPHERIC
$T_o$ = 103° F
PROBE OF TYPE SHOWN IN FIGURE
M=1.2 AHEAD OF SHOCK WAVE
ZERO VELOCITY
D.C. VOLTAGE
400
350
300
0
0
2
4
6
8
10
12
14
16
18
CURRENT IN MA.

FIGURE (29)

0.65 times the atmospheric pressure; this reduction of pressure is favorable to the stability of the glow. Secondly, since the product of the velocity ahead and behind of a normal shock wave is a constant, the velocity in which the glow discharge finds itself decreases as the free stream Mach number is increased.

A typical curve of the direct current voltage across the glow discharge as a function of the free stream Mach number is given as Figure (30). In view of the discussion in the preceding paragraph, it is not surprising to see that the voltage decreases as the Mach number is increased.

A qualitative indication of the response of the glow discharge to the velocity fluctuations in a supersonic air stream was obtained by observing the oscilloscope as the probe was moved into the boundary layer, which was visible on the Schlieren viewing plate. The alternating voltage signal observed on the oscilloscope was of the same general nature as that observed at subsonic velocities, but was at a much higher frequency. As the probe was moved into the boundary layer, this signal was increased about tenfold. The alternating signal was also observed as the probe was traversed through the wake of a 0.014 inch wire which was stretched across the middle of the test section. At a distance of eight centimeters behind the wire, a peak was observed in both the alternating signal and the direct current voltage as the probe passed through the top and bottom of the wake; between these peaks (i.e. directly behind the wire) the voltages dropped to a value about equal to that observed several centimeters above and below the wire. At a distance of 35 centimeters behind the wire, a single smaller voltage peak extending across

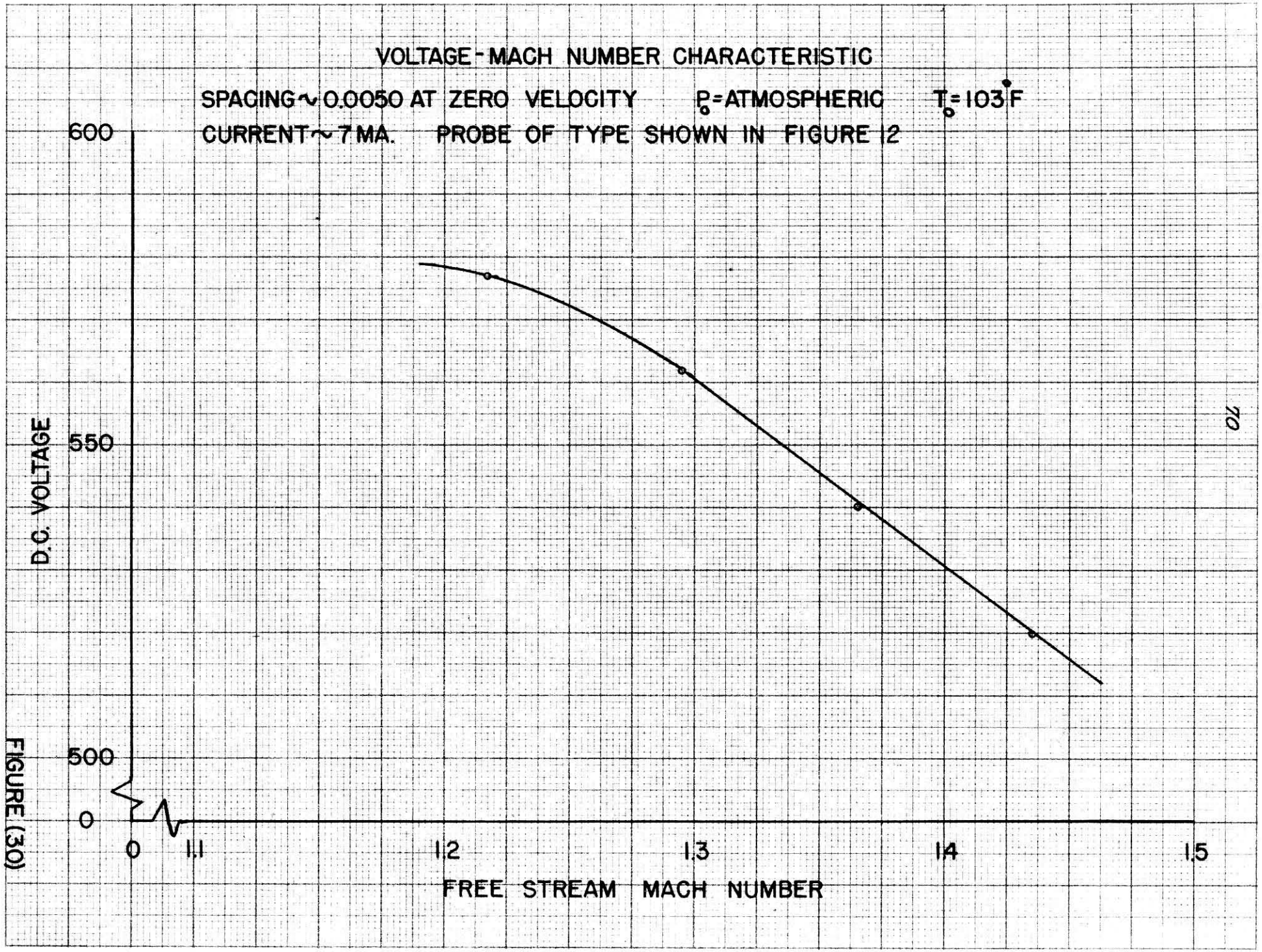
VOLTAGE - MACH NUMBER CHARACTERISTIC
SPACING ~ 0.0050 AT ZERO VELOCITY
P₀ = ATMOSPHERIC
T₀ = 103°F
CURRENT ~ 7 MA.
PROBE OF TYPE SHOWN IN FIGURE 12
600
550
500
0
D.C. VOLTAGE
0
1.1
1.2
1.3
1.4
1.5
FREE STREAM MACH NUMBER
70

FIGURE (30)

the entire wake was observed. It thus appears that the glow discharge responds, at least in a qualitative way, to velocity fluctuations in a supersonic air stream.

## V. CONCLUSIONS; SUGGESTIONS FOR FURTHER RESEARCH

A glow discharge can be maintained and is stable in a transverse air stream at pressures near atmospheric throughout the subsonic velocity range, and at supersonic air velocities up to a Mach number of 1.5; there are no indications that this Mach number represents the upper limit of the velocities at which stable operation is possible. With the current held constant, the direct current voltage across the glow discharge responds quantitatively and in a reproducible manner to velocity changes with a sensitivity depending chiefly upon the spacing between the electrodes. The pressure and temperature changes accompanying velocity changes and the aerodynamic forces affect the electrode spacing and therefore the voltage, but their effect was shown to be of second order importance compared to the effect of velocity changes.

A calibration procedure has been developed for the glow discharge anemometer and was used in measuring the decay of turbulence behind a grid at low subsonic velocities. Comparison with decay measurements made independently with a hot wire anemometer under similar flow conditions showed that the glow discharge data was quite badly scattered and was somewhat inconsistent. This inconsistency, which is probably caused by sputtering of the electrodes, and the problem of controlling the noise level must both be resolved before the glow discharge anemometer can become an accurate instrument. The glow discharge was shown to respond qualitatively to velocity fluctuations in a supersonic air stream.

The technique of operating and calibrating the glow discharge

anemometer is, at present, quite difficult. The physical size of the probe used is comparable to the size of a hot wire anemometer probe. Any probe-type measuring instrument which is inserted into an air stream influences the conditions at the point of measurement. This influence is present at all velocities and complicates the interpretation of the results obtained. At supersonic velocities it takes the spectacular form of a shock wave.

A theory of the dark current discharge anemometer has been developed, and it gives results which agree in form with reported experimental measurements. This theory considers the current decrease of a dark current discharge operated at constant voltage observed as the transverse air velocity is increased, to be directly the result of the loss of those positive ions which are blown out of the discharge space by the air stream. A qualitative theory of the mechanism of the glow discharge anemometer and the first steps of the corresponding quantitative analysis have been developed. This theory considers the voltage increase observed as a glow discharge is operated at constant current and as the transverse air velocity is increased, to be the result of the loss of positive ions from the discharge, and of the re-distribution of the positive ion space charge necessary to allow the glow discharge to sustain itself. The loss of positive ions from the glow discharge in a high speed air stream was observed visually.

It is evident at this point that a considerable amount of additional research is necessary before the glow discharge anemometer or any gas discharge anemometer will be a useful tool in fluid mechanics research. The key to the improvement of the glow discharge anemometer

appears to be a better understanding of sputtering and its effects. A detailed experimental study of sputtering at atmospheric pressure, possibly with an accompanying analysis by the methods of wave mechanics, might indicate a method of reducing the amount of sputtering. The use of an alternating current glow discharge operated at a frequency of the order of kilocycles has interesting possibilities in this connection.

An aerodynamic study of the flow to be expected in the gap between the faces of two coaxial solid cylinders separated by a short spacing and placed in a transverse air stream in which the size of the turbulent eddies is of the order of the spacing, would provide some of the background knowledge necessary to properly design the glow discharge anemometer probes. The results of such a study, together with a better knowledge of sputtering, would probably explain the unduly large and erratic alternating voltages sometimes obtained in an apparently turbulence-free air stream.

A quantitative study of the relationship between the current and voltage of an arc discharge operated in a transverse air stream at currents of the order of amperes might prove useful in the design of air blast circuit breakers.

APPENDIX A

The integral equation (equation (14)) derived to enable solving for the number of electrons leaving various points on the cathode per square centimeter per second was:

$$n_c(y) = n_o + \gamma \int_{y-\frac{vL}{\mu_p E}}^{y} \frac{\alpha \mu_p E}{v} n_c(y_1)\, e^{\frac{\alpha \mu_p E}{v}(y-y_1)}\, dy_1 \qquad (14)$$

where the coordinates and dimensions are defined as shown by Figure (2). Under the stated assumptions, $\alpha, \mu_p, E, \gamma$, and $v$ are all constants. The function $n_c(y)$ must be finite and continuous in the range $0<y<h$, must reduce to $n_o$ when y is zero, and is zero for negative values of y.

For values of y less than $\frac{vL}{\mu_p E}$ the lower limit of the integral in equation (14) is negative, and may be set equal to zero, since $n_c(y_1)$ is zero for negative values of y. Thus, for $0<y<\frac{vL}{\mu_p E}$,

$$n_c(y) = n_o + \frac{\gamma \alpha \mu_p E}{v} \int_0^y n_c(y_1)\, e^{\frac{\alpha \mu_p E}{v}(y-y_1)}\, dy_1 \qquad (34)$$

which is a Volterra integral equation of the second kind. Treating the integral on the right side as a convolution integral, one can take the Laplace transform of both sides, and obtain, using s for the complex variable,

$$n_c(s) = \frac{n_o}{s} + \frac{\gamma \alpha \mu_p E}{v} n_c(s) \frac{1}{s - \frac{\alpha \mu_p E}{v}} . \qquad (35)$$

Solving for $n_c(s)$, one then obtains,

$$n_c(s) = \frac{n_o\left(s - \frac{\alpha\mu_p E}{v}\right)}{s\left(s - (1+\gamma)\frac{\alpha\mu_p E}{v}\right)} \quad . \tag{36}$$

Taking the inverse transform, one arrives at the solution for $n_c(y)$, for $o < y < \frac{vL}{\mu_p E}$, which was given as equation (15),

$$n_c(y) = \frac{n_o}{1+\gamma}\left(1 + \gamma e^{\frac{\alpha\mu_p E}{v}(1+\gamma)y}\right) . \tag{15}$$

A solution for the range $\frac{vL}{\mu_p E} < y < \frac{2vL}{\mu_p E}$ can now be obtained. To save re-writing the groups of constants which occur in these equations, let equation (14) be written in the form,

$$n_c(y) = a + b\int_{y-d}^{y} n_c(y_1)\cdot e^{c(y-y_1)}\, dy_1 \tag{37}$$

where the values of a, b, c, and d are easily determined by direct comparison with equation (14). Differentiating both sides of this equation, with respect to y,

$$\frac{dn_c(y)}{dy} = bc\int_{y-d}^{y} n_c(y_1)\, e^{c(y-y_1)}\, dy_1 - be^{cd} n_c(y-d) + b n_c(y) \tag{38}$$

which by using equation (37) can be re-written as,

$$\frac{dn_c(y)}{dy} = c\left(n_c(y) - a\right) - be^{cd} n_c(y-d) + b\, n_c(y) \tag{39}$$

Collecting terms,

$$\frac{dn_c(y)}{dy} = (b+c)\, n_c(y) - ac - be^{cd} n_c(y-d) \tag{40}$$

In the range $\frac{vL}{\mu_p E} < y < \frac{2vL}{\mu_p E}$, the function $n_c(y-d)$ where $d = \frac{vL}{\mu_p E}$ is known from our solution for $n_c(y)$ in the range $o < y < \frac{vL}{\mu_p E}$. In terms of the constants a, b, and c the solution in this lower range is,

$$n_c(y) = \frac{a}{c+b}\left(c + b e^{(c+b)y}\right) \tag{41}$$

One therefore obtains for equation (40),

$$\frac{dn_c(y)}{dy} = (b+c)\,n_c(y) - ac - be^{cd}\left(\frac{ac}{c+b} + \frac{ab}{c+b}e^{(c+b)(y-d)}\right) \tag{42}$$

which is a linear equation and can readily be integrated. Using $e^{-(b+c)y}$ as an integrating factor, and employing the condition that at $y = \frac{Ul}{\mu_p E}$, the solutions for y greater and less than $\frac{Ul}{\mu_p E}$ must be identical, one obtains for $\frac{Ul}{\mu_p E} < y < \frac{2Ul}{\mu_p E}$,

$$n_c(y) = \frac{ac}{c+b} + \frac{abc}{(c+b)^2}e^{cd} + \left\{\frac{ab}{c+b} + \frac{ab^2d}{c+b}e^{-bd} - \frac{abc}{(b+c)^2}e^{-bd}\right\}e^{(b+c)y} - \frac{ab^2e^{-bd}}{c+b}\,y\,e^{(b+c)y} \tag{43}$$

Substituting the values of a, b, c, and d,

$$n_c(y) = \frac{n_o}{1+\gamma} + \frac{n_o\gamma e^{\alpha l}}{(1+\gamma)^2} + \left\{\frac{n_o\gamma}{1+\gamma} - \frac{n_o\gamma e^{-\gamma\alpha l}}{(1+\gamma)^2} + \frac{n_o\gamma^2\alpha l}{(1+\gamma)}e^{-\gamma\alpha l}\right\}e^{\frac{\alpha\mu_p E}{U}(1+\gamma)y} - \frac{n_o\gamma^2\alpha\mu_p E}{U(1+\gamma)}e^{-\gamma\alpha l}\,y\,e^{\frac{\alpha\mu_p E}{U}(1+\gamma)y} \tag{44}$$

which is the solution given as equation (16). By direct substitution, equations (15) and (16) can be shown to satisfy the original integral equation. The limiting conditions can be checked by noting that the solution in the lower range approaches $n_o$ as y approaches zero, which is proper, and that both solutions converge to the same value as y approaches their common point $\frac{Ul}{\mu_p E}$. It will be observed that as the velocity $U$ is allowed to approach zero, the solution for the lower range does not directly approach the solution for zero velocity obtained previously. (Equation (21)). This is not surprising since the range

of validity, $0 < y < \frac{VL}{\mu_p E}$, of the solution in the lower range also approaches zero as $V$ approaches zero.

If the solution $n_c(y)$ is needed for $y > \frac{2VL}{\mu_p E}$ it can be obtained by the same method as was used above. It is only necessary to restrict the variable successively to the ranges $\frac{2VL}{\mu_p E} < y < \frac{3VL}{\mu_p E}$, $\frac{3VL}{\mu_p E} < y < \frac{4VL}{\mu_p E}$, etc. At each step in the continuation process, the term $n_c(y-d)$ is known from the solution in the previous range.

## APPENDIX B

The current $I_G$ flowing in the ground wire as shown in Figure (3) must, if the potential level of the entire circuit is to remain constant, equal the number of ions blown out of the discharge per second, multiplied by the charge per ion. Therefore, the relation,

$$I_G = I_A - I_c = q \left\{ \begin{array}{l} \text{Number of ions} \\ \text{blown out per second} \end{array} \right\} \tag{45}$$

must be true. This relation can be checked by directly evaluating the number of ions blown out of the discharge, and comparing with $(I_A - I_c)$. The number of ions blown out of the discharge per second in the steady state is just the number produced per second in the space labeled ABCD of Figure (3). For the air velocity, field strength, and electrode width illustrated in Figure (3) this number is given by,

$$N_L = \int_0^{\frac{h\mu_p E}{v}} \alpha e^{\alpha x} \left[ \int_{h-\frac{vx}{\mu_p E}}^{h} n_c(y)\, dy \right] dx + \int_{\frac{h\mu_p E}{v}}^{L} \alpha e^{\alpha x} \left[ \int_0^h n_c(y)\, dy \right] dx . \tag{46}$$

This expression can be re-written as,

$$N_L = \int_0^{\frac{h\mu_p E}{v}} \alpha e^{\alpha x} \left[ \int_0^h n_c(y)\, dy - \int_0^{h-\frac{vx}{\mu_p E}} n_c(y)\, dy \right] dx + \int_{\frac{h\mu_p E}{v}}^{L} \alpha e^{\alpha x} \left[ \int_0^h n_c(y)\, dy \right] dx . \tag{47}$$

By properly combining these integrals one obtains,

$$N_L = \int_0^{L} \alpha e^{\alpha x} \left[ \int_0^h n_c(y)\, dy \right] dx - \int_0^{\frac{h\mu_p E}{v}} \alpha e^{\alpha x} \left[ \int_0^{h-\frac{vx}{\mu_p E}} n_c(y)\, dy \right] dx . \tag{48}$$

By interchanging the order of integration on the first integral, and performing the x integration, the expression becomes,

$$N_L = (e^{\alpha L} - 1)\int_0^h n_c(y)\,dy - \int_0^{\frac{h\mu_p E}{U}} \alpha e^{\alpha x}\left[\int_0^{h-\frac{Ux}{\mu_p E}} n_c(y)\,dy\right] dx \quad . \qquad (49)$$

Examining this expression, the first term on the right is seen to be the number of ions produced per second in the entire discharge; the second term is just the number produced per second in the space ADE (See Figure (3)), and is therefore the number which strike the cathode per second. Their difference is clearly the number blown out of the discharge per second. Writing now, from equations (17) and (19),

$$I_A - I_c = q e^{\alpha L}\int_0^h n_c(y)\,dy - q\int_0^h n_c(y)\,dy - q\int_0^h n_p(y)\,dy \qquad (50)$$

and collecting terms,

$$\frac{I_A - I_c}{q} = (e^{\alpha L} - 1)\int_0^h n_c(y)\,dy - \int_0^h n_p(y)\,dy \qquad (51)$$

The first term on the right of this expression is equal to the first term of equation (49) and is the number of ions produced in the discharge per second; the second term is simply the number of ions striking the cathode per second. Hence $\frac{I_A - I_c}{q}$ is clearly the number of ions blown out of the discharge per second.

As examples of equations (17) and (20), take the case where the air velocity, field strength, electrode spacing, and electrode width are such that $\frac{UL}{\mu_p E} > h$ . Then $n_c(y)$ in the first range, $0 < y < \frac{UL}{\mu_p E}$ ,

applies to the entire cathode, and the anode current becomes,

$$I_A = \frac{n_o h q e^{\alpha L}}{1+\gamma} + \frac{q n_o \gamma U e^{\alpha L}}{(1+\gamma)^2 \alpha \mu_p E} \left( e^{\frac{\alpha \mu_p E}{U}(1+\gamma)h} - 1 \right) \quad (52)$$

and the cathode current becomes,

$$I_c = \frac{n_o U q}{(1+\gamma)\alpha \mu_p E} \left( e^{\frac{\alpha \mu_p E}{U}(1+\gamma)h} - 1 \right) . \quad (53)$$

It will be seen that these expressions satisfy equation (22). By dividing by the value of current for zero velocity given by equation (21), one obtains,

$$\frac{I_A}{I_o} = (1+\gamma-\gamma e^{\alpha L}) \left\{ \frac{1}{1+\gamma} + \frac{U\gamma}{(1+\gamma)^2 h \alpha \mu_p E} \left[ e^{\frac{\alpha \mu_p E}{U}(1+\gamma)h} - 1 \right] \right\} \quad (54)$$

and,

$$\frac{I_c}{I_o} = \frac{(1+\gamma-\gamma e^{\alpha L})\ U}{(1+\gamma)\, h \alpha \mu_p E\, e^{\alpha L}} \left[ e^{\frac{\alpha \mu_p E}{U}(1+\gamma)h} - 1 \right] . \quad (55)$$

Although it would be algebraically complicated, equations (54) and (55) could be solved for the voltage across the discharge at constant current if such information were desired. One would simply set $E$ equal to $\frac{V}{L}$ and $\alpha$ equal to the approximate expression $Ap\, e^{\frac{Bpd}{V}}$ and solve for the voltage $V$. The constants A and B for various gases are tabulated in references (4) (5) and (6).

## LIST OF SYMBOLS

$\alpha$ - first Townsend coefficient.

$\gamma$ - average number of electrons released at any point on the cathode per bombarding positive ion.

$E$ - electric field strength.

$h$ - electrode width.

$L$ - electrode separation.

$\mu_e$ - electron mobility.

$\mu_p$ - positive ion mobility.

$n_c$ - total number of electrons leaving any point on the cathode per unit area per second.

$n_e$ - number of electrons crossing a unit area per second.

$n_o$ - number of electrons leaving the cathode per unit area per second as a result of excitation from outside the discharge.

$n_p$ - number of positive ions striking any point on the cathode per unit area per second.

$s_2$ - distance along the electron paths.

$U$ - mean air velocity.

$\phi$ - angle by which ion paths are inclined from the x axis.

$x$ - coordinate perpendicular to the air flow direction.

$x_1, x_2$ - running coordinates in the x-direction.

$y$ - coordinate in the direction of the air flow.

$y_1, y_2$ - running coordinates in the y-direction.

REFERENCES

(1) F. C. Lindvall, "A Glow Discharge Anemometer", A.I.E.E. Trans. (1934), Vol. 53, pages 1068-1073.

(2) These microfilms are currently indexed in the "Cumulative Author Index of the Desk Catalog of German and Japanese Air Technical Documents" under the names of W. Fucks and F. Kettel; this index is issued and the microfilms are distributed by the Headquarters Air Materiel Command, Wright-Patterson Air Force Base, Dayton, Ohio.

(3) W. Fucks, "Investigation of the Operating Properties of the Leakage Current Anemometer"; translated by the N.A.C.A. and issued as T. M. 1178 (1947).

(4),(7) L. B. Loeb, Fundamental Processes of Electrical Discharge in Gases, Wiley and Sons (1947), pages 5, 191.

(5) J. D. Cobine, Gaseous Conductors, McGraw-Hill (1941).

(6) A. V. Engel and M. Steenbeck, Electrische Gasentladungen, ihre Physik und Technik, two volumes, J. Springer (1934).

(8) W. Fucks, "Ueber die Eignung der Vorstromentladung zur Messung von Stromungsgeschwindigkeiten von Gasen (Vorstromanemometer)", microfilm, document number ZWB/THA/70. (See reference (2)).

(9) F. Kettel, "Proprietes de la Sonde Ionique en vue des Applications", translated into French from German and issued as report number 8/45 of the Laboratoire de Recherches balistiques et aerodynamiques, Annexe de Saint-Louis, Saint-Louis, France.

(10) T. Phillips, "A Diaphragmless Microphone for Radio Broadcasting", A.I.E.E. Trans. (1923), Vol. 42, pages 1111-14.